Universidade Federal de Ouro Preto

Núcleo de Pesquisa em Ciências Biológicas

Programa de Pós-Graduação em Ciências Biológicas
PPG CBIOL

Dissertação

Study of the role of the membrane protein caveolin-1 on *Zika virus* replication inside THP-1 cells.

Alejandra Carla Rojas Coronel

Ouro Preto
2019

UFOP

Departamento de Ciências Biológicas - DECBI

Laboratório de Biologia e Tecnologia de Microrganismos – LBTM

Núcleo de pesquisas em Ciências Biológicas - NUPEB

Universidade Federal De Ouro Preto – UFOP

Study of the role of the membrane protein caveolin-1 on Zika virus replication inside THP-1 cells

Ouro Preto

2019

Dissertation presented to the Postgraduate Program in Biological Sciences ('Programa De Pos-Graduação Em Ciências Biológicas – CBIOL') of the Research Center of Biological Sciences ('Núcleo De Pesquisas Em Ciências Biológicas – NUPEB') of the Universidade Federal de Ouro Preto, as a requirement to obtain the degree of Masters in Biological Sciences ('Mestrado em Ciências Biológicas').

Area of concentration – Structural Biochemistry and Molecular Biology.

Author: Alejandra Carla Rojas Coronel

Supervisor: Prof. Dr. Breno de Mello Silva

R741s Rojas, Alejandra.
Study of the role of the membrane protein c aveolin-1 on Zika virus replication inside THP-1 cells [manuscrito] / Alejandra Rojas. - 2019.
73f.: il.: color; grafs; tabs.

Orientador: Prof. Dr. Breno de Mello Silva.

Dissertação (Mestrado) - Universidade Federal de Ouro Preto. Instituto de Ciências Exatas e Biológicas. Núcleo de Pesquisas em Ciências Biológicas. Programa de Pós-Graduação em Ciências Biológicas.
Área de Concentração: Bioquímica Estrutural e Biologia Molecular.

1. Vírus da Zika. 2. Proteínas. 3. Lipídios. I. Silva, Breno de Mello . II. Universidade Federal de Ouro Preto. III. Titulo.

CDU: 577.112/.115

Catalogação: www.sisbin.ufop.br

MINISTÉRIO DA EDUCAÇÃO
UNIVERSIDADE FEDERAL DE OURO PRETO
PROGRAMA DE PÓS-GRADUAÇÃO EM CIÊNCIAS BIOLÓGICAS

UFOP

ATA DE DEFESA DE DISSERTAÇÃO

Aos 06 dias do mês de novembro do ano de 2019, às 09:00 horas, nas dependências Núcleo de Pesquisas em Ciências Biológicas (Nupeb), foi instalada a sessão pública para a defesa de dissertação da mestranda **Alejandra Carla Rojas Coronel**, sendo a banca examinadora composta pelo Prof. Dr. Breno de Mello Silva (Presidente - UFOP), pelo Prof. Dr. Luiz Felipe Leomil Coelho (Membro - Externo), pelo Prof. Dr. Roberto Farina de Almeida (Membro - UFOP). Dando início aos trabalhos, o presidente, com base no regulamento do curso e nas normas que regem as sessões de defesa de dissertação, concedeu à mestranda 30 minutos para apresentação do seu trabalho intitulado "Study of the Role of Caveolin-1 on Zika Virus Replication in Thp-1 Cells", na área de concentração: Bioquímica Estrutural e Biologia Molecular. Terminada a exposição, o presidente da banca examinadora concedeu, a cada membro, um tempo máximo de 45 minutos para perguntas e respostas à candidata sobre o conteúdo da dissertação, na seguinte ordem: Primeiro, Prof. Luiz Felipe Leomil Coelho; segundo, Prof. Roberto Farina de Almeida; terceiro, Prof. Breno de Mello Silva. Dando continuidade, ainda de acordo com as normas que regem a sessão, o presidente solicitou aos presentes que se retirassem do recinto para que a banca examinadora procedesse à análise e decisão, anunciando, a seguir, publicamente, que a mestranda foi aprovada por unanimidade, sob a condição de que a versão definitiva da dissertação deva incorporar todas as exigências da banca, devendo o exemplar final ser entregue no prazo máximo de 60 (sessenta) dias à Coordenação do Programa. Para constar, foi lavrada a presente ata que, após aprovada, vai assinada pelos membros da banca examinadora e pela mestranda. Ouro Preto, 06 de novembro de 2019.

Breno de Mello Silva
Prof. Dr. Breno de Mello Silva
Presidente

XXXXXXXXXXXXXXXXXXXXXXXXXXXX
Prof. Dr. Luiz Felipe Leomil Coelho
(Participação por Videoconferência)

Prof. Dr. Roberto Farina de Almeida

Alejandra Rojas
Mestranda

Certifico que a defesa realizou-se com a participação a distância do(s) membros(s) Prof. Dr. Luiz Felipe Leomil Coelho e que, depois das arguições e deliberações realizadas, cada participante a distância afirmou estar de acordo com o conteúdo do parecer da banca examinadora, redigido nesta ata.

Breno de Mello Silva
Prof. Dr. Breno de Mello Silva
Presidente

DEDICATORY

This dissertation is dedicated to my family who always supported me and to all my professors and researchers in Venezuela, my home country, who encouraged the spark of science in me and are continuously forming generations of professionals regardless of all difficulties.

ACKNOWLEDGMENTS

Foremost, I would like to express my sincere gratitude to my advisor Prof. Breno de Mello Silva for the continuous support of my Master study and research, for his patience, motivation and knowledge. His guidance helped me in all the time of research and writing of this dissertation.

Besides my advisor, my sincere thanks also goes to Prof. Prof. William de Castro Borges and his wife Dr. Renata Alves de Oliveira e Castro for their trust and unconditional support that allowed us, my husband and I, to come to Brazil from Venezuela to do science.

I thank all my fellow lab mates in the Laboratory of Biology and Technology of Micro-organisms (LBTM), specially to Natália Mendes, Ricardo Lemes, Cyntia Ferreira, Leticia Trinidade and Ariane Ferraz, for the stimulating discussions, disposition and support over the last two years. I also thank my friends, Nauhara Castro, Mariane Luyara and Igor Aparecido for the moral support that made it possible for me to complete this project. I extend my thanks to all concerned persons who co-operated with me in this regard.

I submit my heartiest gratitude to my family, my father Carlos Alberto Rojas Brandi and my mother Milagros Coromoto Coronel de Rojas who have always believed in me, their passionate encouragement for me to chase my dreams are a fundamental base for everything that I do. Thanks to all my siblings: Carlos Alejandro, Anyella and Carlos Alberto Rojas Coronel for your moral teachings, affection and emotional backing during the development of my Masters Project.

Last but not least, my joy knows no bounds in expressing my gratefulness to my dear husband, Miguel Cosenza. Thank you for all the inspiration and support you gave me since the very first moment I met you 10 years ago. Your friendship and love gave me all the strength that I ever needed to complete this journey.

To the funding sources, the ‘Coordenação de Aperfeiçoamento de Pessoal de Nível Superior’ (CAPES – Finance code 001) and FAPEMIG for the scholarship and resources to develop this research.

EPIGRAPH

"It is impossible to convey completely the excitement of discovery, of seeing the result of an experiment and knowing that you know something new, something fundamental, and that for this moment at least, only you, in the entire world, knows it"

- Stuart Firestein

ABSTRACT

Zika virus (ZIKV) is an arthropod-borne Flavivirus that affect millions of people worldwide. Its genome is composed of a single-stranded positive RNA that encodes 10 known proteins. It can be transmitted by mosquitos of the *Aedes* genus, as well as by sexual intercourse and blood transfusion. Although the symptoms of acute ZIKV infection are usually mild and self-limited, it causes microcephaly in fetuses of pregnant women, and Guillian–Barré syndrome in adults. Since no treatment or vaccine has been developed until today, further studies are needed to characterize the interaction between ZIKV proteins and host cells. Recent studies have shown that lipid rafts are known to be preferred sites for interaction between viruses and host cells, which may trigger molecular signaling to favor virus multiplication. Caveolae lipid rafts are a subset of membrane rafts, which molecular marker is caveolin-1 protein, since is the responsible for caveolae formation. They are cellular domains that concentrate plasma membrane proteins and lipids involved in the regulation of cell function, which serve as an organizing center for biological phenomena and cellular signaling. Caveolae lipid rafts involvement in ZIKV processing, replication, and assembly remains poorly characterized. Here, we hypothesized a potential implication of caveolin-1 protein in the replication process for ZIKV inside the cell. This was evaluated by measuring the effect of ZIKV infection on cav-1 expression. Then, it was also studied the effect of lipid raft removal with β-methyl cyclodextrin (β-MCD) and both silencing and overexpression of cav-1, on viral multiplication, using qrt-PCR to detect ZIKV mRNA load on the cell. A decreased of cav-1 expression was observed after infection, suggesting a possible virus modulating role. Furthermore, when cellular cholesterol was depleted by β-MCD treatment after ZIKV entrance, lipid rafts were disrupted and virus genome copies were reduced inside the cell. Additionally, neither cav-1 silencing nor overexpression showed any consistent effect on ZIKV replication. These data suggest an important role of caveolar cholesterol-rich lipid raft microdomains in ZIKV replication, nevertheless further studies need to be made to confirm a specific effect of cav-1 over ZIKV multiplication.

Keywords: Zika virus, caveolin-1, lipid rafts.

List of Figures

List of tables

List of abbreviations

THP-1: Tohoku Hospital Pediatrics-1 (human leukemic monocytes cells)

ZIKV: Zika Virus

YFV: Yellow Fever Virus

DENV: Dengue Virus

JEV: Japanese Encephalitis Virus

WNV: West Nile Virus

GBS: Gillian Barre Syndrome

ssRNA(+): positive single stranded RNA

dsRNA: double stranded RNA

mRNA: Messenger RNA

shRNA: short hairpin RNA

ER: Endoplasmic Reticulum

kb: kilobases

bp: base pair

M.O.I.: Multiplicity of infection

HMGCR: 3-hydroxy-3-methyl-glutaryl-coenzyme A reductase

CDs: Cyclodextrins

MβCD: Methyl β-ciclodextrins

CAV-1: caveolin-1

MAPK: Mitogen-Activated Protein Kinases

PI3: Phosphatidylinositol 3

ERK 1/2: Extracellular signal-Regulated Kinases 1/2

AKT: Protein Kinase B

ATM-ATR: Serine/threonine-protein kinase - ataxia telangiectasia protein

PKA: Protein kinase A

AMPK: AMP-activated protein kinase

JNK: c-Jun N-terminal kinases

P38 MAPK: p38 Mitogen-Activated Protein Kinases

NFKβ: Nuclear factor kappa-light-chain-enhancer of activated B cells

JAK/STAT3: Janus kinase/Signal transducer and activator of transcription proteins

IL-6: Interleucin-6

G/C and A/U: guanine/cytosine and adenine/uracil

Table of content

1 Introduction

1.1 General aspects of ZIKV

1.1.1 History and classification

The ZIKV was discovered in the course of a study of the vector responsible for the cycle of sylvan YFV in Uganda in 1947. The first human ZIKV isolate came from a 10-year-old Nigerian female in 1954. Outside Africa, ZIKV was isolated for the first time from mosquitoes *Aedes aegypti* (*A. aegypti*) in 1969 in Malaysia; subsequently, the first human infections were reported in Indonesia, in 1977. The virus spread to the Pacific region in 2007, where firstly emerged at the Federated States of Micronesia (Western Pacific), then in 2013, it was found in French Polynesia (South Pacific) (MUSSO; GUBLER, 2016). Finally, in 2015 the first Zika fever was confirmed in Brazil and subsequently, autochthonous ZIKV circulation was reported in 12 other countries and territories of the Americas (HENNESSEY et al., 2016).

In the Caribbean as in Europe and EEUU were only reports of imported cases on travelers (ZHONG et al., 2016).

ZIKV was classified inside the *Flavivirus* genus of the Flaviviridae family, which includes a number of medically important arboviruses such as Yellow Fever Virus (YFV), Dengue Virus (DENV), Japanese Encephalitis Virus (JEV) and Western Nile Virus (WNV) (SIMMONDS et al., 2017).

1.1.2 ZIKV structure

Structurally, ZIKV is similar to other flaviviruses. The virus particle has an overall average size of 45–75 nm and the nucleocapsid is surrounded by a host membrane-derived lipid bilayer that contains envelope (E) and membrane (M) proteins arranged in an icosahedral-like symmetry containing a ssRNA(+) viral genome of approximately 10.7 kb (LEE et al., 2018).

The genomic RNA is flanked by two terminal non coding regions, which includes a single large open reading frame encoding a polyprotein. This polyprotein is processed by viral and host proteases that will produce a total of ten mature viral proteins: three structural proteins (C, M, and E) and seven nonstructural (NS1, NS2A,

NS2B, NS3, NS4A, NS4B, and NS5) proteins that will make up the viral replication complex for virus replication (CHAMBERS et al., 1990).

1.1.3 ZIKV life cycle

The ZIKV infectious cycle starts with the virus binding to host cell surface receptors and attachment factors via the E protein, leading to clathrin-dependent endocytosis. Internalized virus particles fuse with the endosomal membrane in a pH-dependent manner, releasing the genomic RNA into the cytoplasm of the host cell (SAGER et al., 2018).

Viral replication takes place in intracellular membrane-associated compartments, called lipid rafts, located on the surface of the endoplasmic reticulum (ER), resulting in a dsRNA genome synthesized from the genomic ssRNA(+) by viral RNA polymerase. The dsRNA genome is subsequently transcribed and replicated, resulting in additional viral mRNAs/ssRNA(+) genomes (LEE et al., 2018).

Immature virus particles are assembled within ER then they are then transported through the trans-Golgi network where the fully mature infectious virus particles are formed as soon as prM is processed to M by a Furin-like protease. The new virus particles are released into the extracellular environment where they move on to a new infectious life cycle (GARCIA-BLANCO et al., 2016).

1.1.4 ZIKV transmission and clinical manifestations.

Although ZIKV was first discovered in 1947, it had little attention due to an association with only mild symptom, until this last decade. At some point during its migration from Africa to Asia and then the Pacific Islands, the virus mutated changing the manifestations of its infection (VENTURI et al., 2019). Not only has become more pathogenic, causing Guillain-Barré Syndrome and congenital malformations, but it has acquired alternate routes of transmission not seen in any other mosquito-borne virus (ABECASIS et al., 2019; GUTIÉRREZ-BUGALLO et al., 2019).

ZIKV is primarily transmitted to mammalian hosts by mosquito vectors from the *Aedes* genus, mainly through *A. aegypti*. Nevertheless, transmission can also occur

from blood contact via blood or organ transfusion, and also from mother to child via placenta–fetal transmission (BIPHENYLS, 2015).

Illness resulting from ZIKV infection is typically mild and self-limiting. The majority (approximately 80%) of ZIKV infections have been estimated to be asymptomatic. However, since 2013, an increased incidence of neurological symptoms following ZIKV acute infection, including the GBS, has been reported. Furthermore, the emergence of ZIKV in the Americas coincided with increased reports of babies born with brain malformations (ZANLUCA; DOS SANTOS, 2016).

The adverse pregnancy outcomes from the infection of the mother with ZIKV consist of increased risk of premature delivery, fetal death and miscarriage, and congenital malformations collectively characterized as congenital Zika syndrome, including microcephaly, abnormal brain development, limb contractures, eye abnormalities, brain calcifications, and other neurologic manifestations (ALVARADO; SCHWARTZ, 2017; CAMARGOS et al., 2019).

1.1.5 ZIKV epidemiology

Worldwide, 61 countries have confirmation of established competent *A. aegypti* vectors without documented ZIKV transmission until present. It is also possible that some of these countries have transmission that has not yet been detected or informed; furthermore, 87 countries have or have had confirmed cases of ZIKV transmission, besides, all areas with prior reports of ZIKV transmission have the potential for re-emergence or re-introduction (WHO, 2019).

There is still the potential risk for ZIKV to spread to additional countries due to climate change, uncontrolled use of insecticides, perturbations of natural systems consequences of human activity, expansion of the geographic distribution of mosquito vectors, global growth of human populations with extensive urbanization, lack of effective mosquito control and increased travel (RYAN et al., 2018).

1.1.6 ZIKV treatment

Currently, no vaccines or antiviral treatments have been approved to cure ZIKV infection and patients care is mainly focused on treating their symptoms (MUSSO; GUBLER, 2016).

The best way to prevent ZIKV infection is to avoid mosquito bites by using air conditioning or window and door screens when indoors, wearing long sleeves and pants, and using insect repellents when outdoors (HENNESSEY et al., 2016)

1.2 Importance of lipids rafts present on host cells on Flavivirus biology

The relationship between ZIKV proteins and host cellular responses during infection is still unclear and the study of the role of lipids rafts on ZIKV infection could be an important point to study the interactions between virus and host molecular signaling that favors virus multiplication.

Much of the evidence reported using several methods and model systems suggests that cholesterol distribution in the membrane is heterogeneous and that it is concentrated in rich lipids domains, with a recent consensus membrane rafts definition of “small (10–200 nm), heterogeneous, highly dynamic, sterol and sphingolipid enriched domains that compartmentalize cellular processes” (SIMONS; SAMPAIO, 2011)

Recent studies have shown that lipid rafts are known to be preferred sites for interaction between viruses and host cells. The lipid rafts are utilized in the replication cycle of numerous viruses, internalization receptors of many viruses localize to rafts or are recruited there after virus binding (OSUNA-RAMOS; REYES-RUIZ; DEL ÁNGEL, 2018). Arrays of signal transduction proteins found in rafts contribute to efficient trafficking and productive infection. Some viruses are dependent on raft domains for biogenesis of their membranous replication structures. Finally, rafts are often important in virus assembly (UPLA; HYYPIÄ; MARJOMÄKI, 2009).

Particularly, Flavivirus hijacks the host cell machinery to translate viral proteins and initiate viral genome replication. In their replication cycle membrane rearrangements are induced to serve as a support for the assembly of the viral

progeny; this is carried out in the replication complexes on the ER. These assembly sites have a high activity of enzymes such as the cholesterol-synthesizing enzyme, HMGCR, involved in the cholesterol biosynthesis pathway (MACKENZIE; KHROMYKH; PARTON, 2007), which leads to the replication complexes being rich in cholesterol.

After internalization and uncoating of Flavivirus into the host cell, the viral proteins synthesized such as the NS4A protein induces the ER-membrane remodeling to form membrane curvatures (ROOSENDAAL et al., 2006), the HMGCR host enzyme is then associated with the NS4A viral protein to increase the *de novo* synthesis of fatty acids and cholesterol. Double-membrane vesicles are formed in which NS1, NS3, and NS5 proteins and dsRNA are localized and the viral RNA replication occurs (WELSCH et al., 2009).

The finding that lipid rafts are crucial for successful replication of many viruses generated studies using compounds that affect cholesterol content on cell membranes regarding its effect on viral replication, one of those compounds is cyclodextrins (CDs).

CDs are cyclic oligosaccharides consisting of α-(1–4)-linked D-glycopyranose units that can exist in heptamers and are widely used in cell biology to deplete cells of cholesterol (MAHAMMAD; PARMRYD, 2015).

Although they are water soluble, they contain a hydrophobic cavity which may encapsulate various hydrophobic molecules, like cholesterol. In addition, its solubility on water can be significantly improved by using hydrophilic modifications, such as methylations, being methyl-β-cyclodextrins (MβCDs) the highest with affinity for inclusion of cholesterol (AKTEPE; MACKENZIE, 2018).

Clearly, lipid rafts serve as an organizing center for biological phenomena and there are two main types of lipid rafts, flotillin-rich planar lipid rafts and caveolin-rich caveolae rafts, both are able to bind and compartmentalize signaling molecules and regulate their activity (YIN et al., 2016).

The particular characteristic of caveole lipid rafts is that they form invaginations in the cell membranes and this structure concentrate a higher amount of proteins,

thus, they are involved in more signaling pathways than planar lipid rafts. Caveolin-1 (cav-1) protein is the molecular marker for caveolae rafts since they are essential to caveolae formation. Cav-1 is involved in the regulation of cell proliferation, survival and differentiation (CORDERO et al., 2014). Different pathways are regulated by cav-1 in these processes, mainly MAPK, PI3K and cav-1 can act both positively and negatively on these pathways.

Cav-1 also regulates ERK1/2 and Akt signaling proteins preventing or maintaining its activation, respectively. These are pathways that has been extensively investigated in the context of Flavivirus infection (CHENG et al., 2018), for example, DENV participates in liver inflammation by inducing the expression of various chemokines through activating all three MAPK pathways (LEE et al., 2008b). YFV infection induces ERK1/2 activation and ZIKV infection has a profound modulation of AKT, MAPK–ERK and ATM–ATR signaling proteins (SCATURRO et al., 2018).

THP-1 cells are a type of human monocytes that have high levels of lipid rafts in its cellular membrane (GAUS et al., 2005) and present tropism for ZIKV infection, they are also studied as one of the cells responsible for possible trans-placental transmission of the virus (CHAN et al., 2016). Due to all the characteristics present on this cell model, they were picked for the experiments made on this project.

Even though cav-1 regulates signaling pathways that are common to those used by ZIKV replication cycle, lipid rafts involvement in ZIKV processing, replication, and assembly remains poorly characterized.

The concerning developments of the disease, the continuous spreading of the vector around the world and the lack of treatment make it necessary to find ways to stop the spread of this pandemic and ways to preserve the health of unborn children at risk of neurological devastation. Therefore, studying the role of cav-1 in lipid raft during ZIKV infection could help a better understanding of its biology and could guide the development of new antiviral therapies for patients.

2 Objectives

2.1 General:

Evaluation of the role of caveolin-1 membrane protein (cav-1) on ZIKV infection using the *in vitro* human leukemic monocyte (THP-1) cell model.

2.2 Specifics:

1. Analyze the effect of cholesterol removal on viral replication
2. Evaluate the effects of ZIKV on cav-1 mRNA expression
3. Evaluate the ZIKV replication in both cav-1 silencing and over expression systems

3 Methodology

3.1 Materials

Table 1. Cell culture components

Reagents	Company	Catalog number
RPMI-1640 Medium with L –glutamine and sodium bicarbonate (1g/L)	SIGMA	R6504
Dulbecco's Modified Eagle's Medium (DMEM) HG with 4500 mg/L glucose, L-glutamine and sodium bicarbonate (3,7g/L later added)	SIGMA	D5648
Fetal Bovine Serum (FBS)	GIBCO	12657-029
Opti-MEM Reduced Serum Medium	Thermo Fisher	51985070
Penicillin-Streptomycin (P/S)	GIBCO	15140-122
Trypan Blue powder, BioReagent, suitable for cell culture (liquid preparation 4mg/mL, sterile-filtered)	SIGMA	T6146
Trypsin	GIBCO (1:250)	840-7250IM
β-mercaptoethanol	GIBCO	31350010
Dimethyl sulfoxide (DMSO)	SIGMA	D4540

Table 2. Kits used in this study

Kit name	Company	Catalog Number
QIAGEN MIDI PREP	QIAGEN	12243
SV Total RNA Isolation System	PROMEGA	Z3105
DNA clean and concentrator	ZYMO RESEARCH	D40035
Agarose Gel Extraction kit	CELLCO	Dpk-105S
Cholesterol liquiform kit	LABTEST	76-2/100

Table 3. Bacteria culture

Name	Company	Catalog Number
LB broth base	Invitrogen	12780052
Agar	Dinâmica	1323

Table 4. Chemicals and reagents

Name	Company	Catalog Number
Lipofectamine 3000 Transfection reagent	Invitrogen	L3000015
Methyl B-cyclodextrin	SIGMA	C4555-16
Tetracycline HPLC	SIGMA	T3258-256
Isopropanol	Nuclear	0396
Ethanol	Neon	03467
Agarose molecular biology grade	Fisher Scientific	BP160-500
Ethidium bromide		
DNA TaqPol 500U 10X buffer Mg^{2+} Plus	Sinapse Inc	P1011
dNTP mix 10mM	Promega	Refu121B
Blue/orange 6X Loading dye buffer	Promega	61881
100 kb ladder	Kasvi	K9-100L
GeneRuler 1 kb DNA ladder	Life Technologies	SM1331

Table 5. Buffers and solutions

Application	Buffer	Reagents	Absolute amount	Relative amount
DNA electrophoresis	TAE 50X Stock	Tris-base	2,3M	141g
		Glacial acetic acid	1M	28,55 mL
		Ethylenediaminetetraacetic acid (EDTA)	50mM pH 8	9.3g or 50mL of 0,5M EDTA solution
		dH2O	-	Up to 500mL
	TAE 1X working solution	50x TAE buffer	-	50 mL
		dH2O	-	4,5 L
Culture cells	PBS 1X	NaCl	0.137 M	8 g
		Na_2HPO_4	0.01 M	1.44 g
		KH_2PO_4	0.0018 M	240 mg
		dH2O	-	Up to 1L Adjust pH 7,4
	Trypsin	NaCl	0.136M	40g
		KCl	5.4mM	2g
		Glycose	5.5mM	5g
		$NAHCO_3$	6,9mM	2,9g
		Trypsin	0,05%	2,5g
		EDTA	6,8mM	1g
		Red phenol solution 1%	-	2,25mL
		dH2O	-	Up to 5L

Table 6. Primer sequences for rtPCR and probe for qrtPCR

Name	Sequence 5’ -> 3’
AR1F	CGT AGA CTC GGA GGG ACA TC
AR1R	TTT CGT CAC AGT GAA GGT GG
AR2F	ACC CTA AAC ACC TCA ACG ATG
AR2R	CAG ACA GCA AGC GGT AAA AC
GAPDH FOW	TGG GTG TGA ACC ATG AGA AG
GAPDH REV	GAG TCC TTC CAC GAT ACC AAA G
qNS1Z2F	GGA AGG GTG ATC GAG GAA TG
qNS1Z2R	GTT CTT TCC TGG GCC TTA TCT
qZIKV-FOW	CCG CTG CCC AAC ACA AG
qZIKV-REV	CCA CTA ACG TTC TTT TGC AGA CAT
qZIKV-Probe	/56-FAM/AGC CTA CCT /ZEN/TGA CAA GCA GTC AGA CAC TCA A/3ABkFQ/

Table 7. Primer sequences for PCR

Name	Sequence 5’ -> 3’
AR3F	ACG ACT CGA GGC AAC ATC TAC
AR3R	AAG AGC GCC CAA TAC GCA AA
T7	TAA TAC GAC TCA CTA TAG GG
BGH	TAG AAG GCA CAG TCG AGG
M13 FOW	CGC CAG GGT TTT CCC AGT CAC GAC
M13 REV	GGT CAT AGC TGT TTC CTG TG
CAV1-F	TCC TCA GTT CCC TTA AAG CAC
CAV1-R	TGT AGA TTGT TGC CCT GTT CC

Table 8. Sequences of DNA Oligo for RNA silencing of cav-1 protein

Name	Sequence 5’ -> 3’
shCAV1a	**TCGAG**GCAACATCTACAAGCCCAATTCAAAGAGATTGGGCTTGTAGATGTTGCTTTTTTACGCGTA
shCAV1b	**AGCTT**ACGCGTAAAAAAGCAACATCTACAAGCCCAATCTCTTGAATTGGGCTTGTAGATGTTGCC
Caveolin-sh-fow	**GATCC**GCAACATCTACAAGCCCAATTCAAGAGATTGGGCTTGTAGATGTTGCTTTTTTACGCGTA
Caveolin-sh-rev	**AGCTT**AACGCGTAAAAAAGCAACATCTACAAGCCCAATCTCTTGAATTGGGCTTGTAGATGTTGCG

* Boldface type text refers to restriction sites.

Table 9. gblocks used in this study

Name	Use	Sequence 5' -> 3'
gblock caveolina	Insert for pcDNA$_3$ vector	GACCTAG**AAGCTT**GCCAGCATGTCTGGGGGCAAATACGTAGA CTCGGAGGGACATCTCTACACCGTTCCCATCCGGGAACAGGGC AACATCTACAAGCCCAACAACAAGGCCATGGCAGACGAGCTG AGCGAGAAGCAAGTGTACGACGCGCACACCAAGGAGATCGAC CTGGTCAACCGCGACCCTAAACACCTCAACGATGACGTGGTCA AGATTGACTTTGAAGATGTGATTGCAGAACCAGAAGGGACAC ACAGTTTTGACGGCATTTGGAAGGCCAGCTTCACCACCTTCACT GTGACGAAATACTGGTTTTACCGCTTGCTGTCTGCCCTCTTTGG CATCCCGATGGCACTCATCTGGGGCATTTACTTCGCCATTCTCT CTTTCCTGCACATCTGGGCAGTTGTACCATGCATTAAGAGCTTC CTGATTGAGATTCAGTGCATCAGCCGTGTCTATTCCATCTACGT CCACACCGTCTGTGACCCACTCTTTGAAGCTGTTGGGAAAATAT TCAGCAATGTCCGCATCAACTTGCAGAAAGAAATATATCCCTAT GACGTGCCCGACTATGCCTAA**GGATCC**CATATG
gblock ZIKV	Template for standard curve on qrtPCR for viral quantitation	GTTGTAAAACGACGGCCAGTAGGACYAGAGGTTAGAGGAGAC CCCCCGCACAACAACAAACAGCATATTGACGCTGGGARAGACC AGAGATCCTGCTGTCTCTACAGCATCAWTCCAGGCACAGARCG tTCGACGCGCCCTCTTTAACGGACATGTCATGCGAGGTACCAGC CTGCACCCATTCCTCAGACTTTGGGGGCGTCGCCATTATTAAAT ATGCAGTCAGCAAGAAAGGCAAGTGTGCGGTGCATTCGATCC GCTGCCCAACACAAGGTGAAGCCTACCTTGACAAGCAATCAGA CACTCAATATGTCTGCAAAAGAACGTTAGTGGGGTCATAGCTG TTTCCTGTG

* Boldface type text refers to restriction sites

Table 10. Restriction enzymes

Name	Company	Cat. Number	Restriction site	Digested DNA
HINDIII	Thermo Scientific	ER0501	**AAGCTT**	pSingle-tTS-shRNA pSilencer™ 3.1-H1 neo gBlock caveolina-1 pcDNA$_3$™3.1(+)
Xho I	Fermentas	FD0694	**TCGAG**	pSingle-tTS-shRNA
BAMHI	Fermentas	18226	**GGATCC**	pSilencer™ 3.1-H1 neo gBlock caveolina-1 pcDNA$_3$™3.1(+)

3.2 Methods

3.2.1 Cell culture

For experimental assays, cells derived from human monocytes (THP-1) were transferred from liquid nitrogen storage to a 37°C water bath. Once thawed, the cells were removed from the cryogenic vial and centrifuge at 130g for 10 min to take out old freezing media (Fetal Bovine Serum 90% and dimethyl sulfoxide 10%). The cell pellet was then added to 10mL pre-warmed RPMI media in a 25mL flask and incubated overnight under standard conditions (5% CO_2 at 37°C).

RPMI medium contained 10% FBS, β-mercaptoethanol (50µM), penicillin (200U/mL), streptomycin (100µg/mL) and amphotericin B (2.5µg/ml). Cells were split 1:3 twice a week into pre-warmed media.

For viral titration, VERO cells (derived from monkey kidney epithelial cells), were cultured under standard conditions and passaged two or three times per week (on demand). To do that, cells were washed with PBS 1X and trypsinised for 1 minute at 37˚C. Afterwards, a gentle rocking was applied to ensure complete detachment from the plate. The trypsin was inactivated with FBS-containing media (DMEM-HG 5% FBS, penicillin 200U/mL, streptomycin 100µg/mL and amphotericin B 2.5µg/mL), and the detached cells were pipetted up and down to achieve single cell suspensions. Finally, single cells were re-plated at the desired density in fresh medium.

3.2.2 Virus

In order to study the effect of cav-1 level of expression on ZIKV infection, cells were infected with *Zika virus* isolate ZIKV/*H.sapiens*/Brazil/PE243/2015 (GenBank: KX197192).

3.2.3 Bacteria

Escherichia coli XL10-Gold® Ultracompetent Cells from Strategene (Cat. Number: 200314). Ideal for transformation of large DNA molecules with high efficiency cloning.

3.2.4 Vectors

3.2.4.1 Silencing of cav-1 expression in THP-1 cells

Plasmid vector pSingle-tTS-shRNA/cav-1: containing a CMV promoter/enhancer-controlled expression of the tetracycline-controlled regulatory protein, tTS (tetracycline-controlled transcriptional suppressor), a SV40 promoter for episomal replication, ColE1 ori (ColE1 bacterial origin for replication) and Ampr (Ampicillin resistance gene; β-lactamase) (Attachment 8.1).

To design the shRNA, it was generated a 19-base target sequence (GCAACATCTACAAGCCCAA) for caveolin-1 silencing (GeneBank access number: NM_001753). In order to choose this sequence, it was used the RNAi Target Sequence Selector tool available on Clontech's website. The sequence was analyzed with Blast platform to verify similarity and specificity with the caveolin-1 coding sequence in genome and human transcriptome.

Annealed complementary oligonucleotides, named shCAV1a and shCAV1b, were inserted into the pSingle-tTS-shRNA vector. They were designed using the tool available on Clontech's website, following the manual directions (Knockout Single Vector Inducible RNAi System User Manual - Clontech) (Table 8).

pSilencer™ 3.1-H1 neo-shRNA/cav-1: containing Human H1 promoter for constitutive expression in mammal cells, SV40 origin, ColE1 ori and Ampr (Attachment 8.2).

For the target of caveolin-1 silencing, it was used the same 19-base sequence as the one for the inducible knockout, described above. Nevertheless, the complementary oligonucleotides (caveolin-sh-fow and caveolin-sh-rev. Table 8) were re-designed to introduce specific enzyme digestion sites needed for cloning into the vector.

3.2.4.2 Over expression of cav-1.

Plasmid vector pcDNA™3.1(+)/cav-1: containing cytomegalovirus enhancer-promoter for high-level constitutive expression in mammalian cells, SV40 origin, ColE1 ori, T7 prokaryotic promoter and Ampr (Attachment 8.3).

With the aim of increasing the cav-1 expression in THP-1 cells, a gBlock of cav-1 coding sequence was produced using gBlocks® Gene Fragments Entry tool of the Integrated DNA Technologies website (Table 9).

This gBlock was the insert to be introduced into the $pcDNA_3$ vector backbone at the specific restriction enzyme sites.

3.3 Study design and experimental workflow

In order to confirm if lipid rafts were important for ZIKV replication, the cholesterol in the membranes of THP-1 infected cells were removed with MβCD and the amount of viral RNA copies were quantified and compared with control (no treated) cells. Then, it was important to evaluate if inside of the entire protein complex associated to lipid rafts, cav-1 had an imperative role for ZIKV replication. For this, after infection the levels of gene expression of cav-1 were quantified with qrt-PCR. Finally, to study how the virus behaved on different expression levels of cav-1, several cloning systems were generated, and ZIKV viral replication was quantified in each condition by qrt-PCR and plaque assay (Fig. 1).

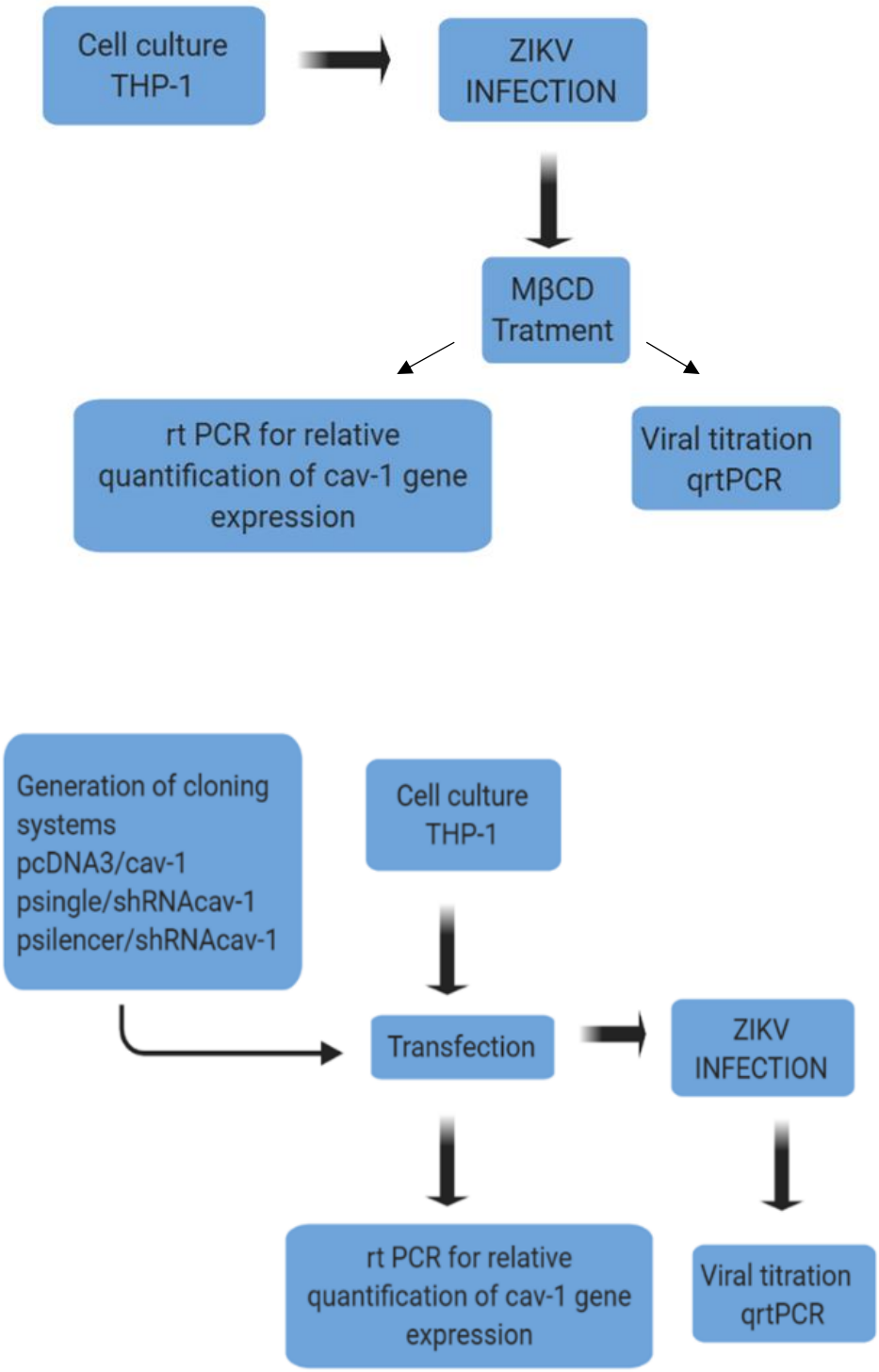

Figure 1. Study design and experimental workflow. Role of caveolae lipid rafts in ZIKV replication by qrt-PCR and viral titration.

3.4 Evaluation of ZIKV infection after lipid rafts depletion.

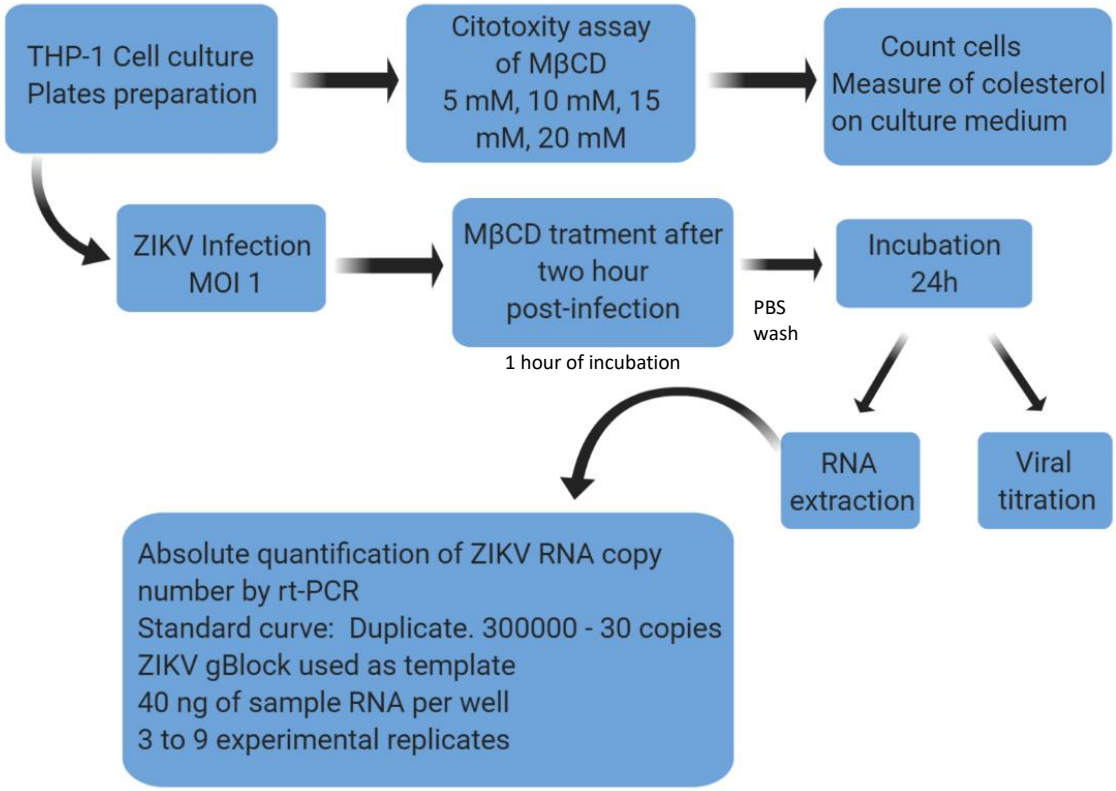

Figure 2. Experimental workflow for evaluation of ZIKV replication after lipid rafts depletion.

3.5 THP-1 cell infection with ZIKV

THP-1 cells were washed with PBS 1X by centrifugation at 130g for 10 min and then inoculated in serum free medium with ZIKV at a M.O.I. 1. The infection proceeded for 1 hour in the stove at standard conditions (5% CO_2 at 37°C) with recurring manual agitation every 10 min. Complete RPMI medium was added, and the cells were incubated at standard conditions for 24h. Infection was made before MβCD treatment to allow an efficient virus entry to the cell (Fig.2).

3.6 Methyl β-cyclodextrin cytotoxicity assay

Toxic effects of MβCD and cholesterol on cells were determined by counting viable cells after treatment with trypan blue exclusion assay, described in section 3.6.1. Cells were cultivated in 6-well plates and incubated with different concentrations of MβCD (5, 10, 15, 20mM) for 1 hour. The cholesterol content was determined by a colorimetric assay the Cholesterol Liquiform kit from Labtest (Brazil), following the manufacturer's instructions.

Briefly, standards and sample tubes were prepared as follows in Table 11:

Table 11. Mix for cholesterol quantification

	Blank	Sample	Pattern
Sample	-----	0,01mL	-----
Pattern (nº 2)	-----	-----	0,01mL
Reagent 1	1,0mL	1,0mL	1,0mL

Tubes were mixed and placed in a 37ºC water bath 10 minutes. The water level in the bath should be higher than the reagent level in the test tubes. The absorbance of each tube was determined at 500 nm by zeroing with blank, using a spectrophotometer UV/VIS. Finally, with the aim of calculating the cholesterol concentration on the culture medium of each condition, a curve was prepared using dilutions of the standard reagents of the kit plotted against the resulting absorbance of each point, which were 1.25, 2.5, 5, 7.5 and 10 mg/dL of cholesterol.

The principle of this enzymatic assay is describe as follows: cholesterol esterase catalyzes the conversion of cholesterol esters to cholesterol and fatty acids. Then cholesterol Oxidase catalyzes the oxidation of cholesterol with production of hydrogen peroxide. The hydrogen peroxide, which is produced stoichiometrically, reacts with 4-aminoantipyrine and phenol generating a chromogen, quinoneimine.

The concentration with least detrimental effects on cells was picked to evaluate ZIKV infection on cells with depletion of lipid rafts.

3.6.1 Trypan blue exclusion assay

The cells were washed after 2 hours of treatment centrifuge at 130g for 10 min. A 1:1 dilution was performed using the 0.4% trypan blue solution. Neubauer's chambers were filled with the resulting suspensions and visualized under light microscope using ×10 magnification. Counting of viable (seen as bright cells) and non-viable cells (stained blue) was performed. Cell viability was calculated in a population of approximately 150 cells.

3.6.2 Cholesterol removal with MβCD from TPH-1 cells

For cholesterol removal, infected cells were washed with PBS 1X and incubated at standard conditions with serum-free RPMI in the absence (control cells) or presence (treated cells) of MβCD (filter sterilized). After 1 hour, the medium was removed and the cells were washed with PBS 1X to remove the β-MCD. Following infection and cholesterol depletion, culture media with virus was harvested to extract viral RNA and quantify viral load by qrt-PCR and also to be tittered by plaque assay as described below. Cells were processed for RNA extraction and viral quantification, described in section 3.8 and 3.9.

3.7 Evaluation of ZIKV multiplication through plaque assay.

Samples were diluted sequentially 10-fold in free serum RPMI medium. Vero cells were cultured on 6- well plates until reach confluence. After one PBS 1X wash, each diluted sample was added to its respective 6-well plate with Vero cell monolayers. Cells were incubated for 1 hour at standard conditions with recurring manual agitation (every 10 min). Cells were washed once with PBS 1X and overlaid with 3 mL of 1, 5% CMC made with 1% FBS DMEM-HG medium.

The plates were incubated at standard conditions for 3 days. Monolayers were then fixed with formaldehyde 10% for 1 hour and stained by adding 2 mL of crystal violet to each well. Virus titer was determined based on the number of plaques in each well and expressed as plate forming units per mL (PFU/mL).

3.8 RNA extraction

RNA was extracted from cell pellets using the SV Total RNA Isolation System (Promega) following the manufacturer's instructions.

For that, cells were collected from the plate and centrifuge at 300g for 5 minutes. The supernatant containing ZIKV was preserved to extract viral RNA following this same procedure. Cells were washed once with ice cold PBS 1X and centrifuged again.

Afterwards, 175µL of Lysis/Binding buffer was added to the washed cells (and supernatant, separately), and vortexed for 15 seconds. The lysate was then diluted with 350µL of dilution buffer and placed in a heated block on 70°C for 3 minutes.

Tubes were centrifuge at 14.000g for 10 minutes and clean supernatant carefully transferred to other tubes, 95% were added and samples carried to spin columns assemblies. The nucleic acids were bound to the column by centrifugation at 14000g for 1 minute.

After centrifugation, the flow through was discarded, and the DNA was digested in the column upon addition of 5µL of DNAseI in 45µL of DNaseI incubation buffer (with $MnCl_2$ cofactor already mixed) for 15 minutes at room temperature.

Past the incubation time, 600µL of Washing Buffer were added to the upper reservoir followed by a 1 minute centrifugation at 14000 g. Then, another washing step were performed by adding 250 µL of the same Washing Buffer followed by a 2 minutes centrifuge at 14000g. Finally, the RNA was eluted by adding 100 µl of Nuclease-Free Water to the membrane and centrifuge at 12000g for 1 minute. The eluted RNA was immediately quantified by NanoDrop Lite Spectrophotometer, noticing that all absorbance measurements at 260/280 ratio were at ~2,0. Then, the RNA could be directly used for RT-PCR or stored at -80˚C for subsequent analysis.

3.9 Evaluation of ZIKV multiplication through quantitative real time PCR (qrt-PCR)

Real time-PCR was used to evaluate and quantify the level of expression of viral infection following treatment. Briefly, RNA extracted from approximately $2x10^5$cells per condition was analyzed by TaqMan® RT-qPCR kit, using the GoTaq® Probe 1-Step RT-qPCR System (Promega). The qPCRs were performed with the Thermocycler 7500 real time PCR System (Applied Biosystems). See section 3.9.2 for reaction mix specifications.

Concentration of viral RNA (copies/mL) was estimated in ZIKV-positive samples by using the standard curve calculated by the 7500 AB instrument. The standard curve was generated in duplicates for each run, by performing 1:10 serial dilutions of gDNA (ZIKV gBlock, see Table 9 for sequence information) to produce five points of 300.000, 30.000, 3.000, 300 and 30 copies, see section 3.9.3 for calculation details. RNA copies of samples were tested using three replicates to assure reproducibility on the experiment.

3.9.1 Primer and probe design

A real-time Primers/Probe set, specific for ZIKV, was synthesized by IDT (Integrated DNA Technologies, Brazil) using the reported sequence of Lanciotti (2008) study. It was used a TaqMan Double-Quenched Probe (5'FAM/ZEN/3'ABkFQ) with two quenchers, ZEN and ABkFQ, and the FAM reporter. The primers and probe sequences are shown in Table 6.

3.9.2 Taqman qrt-PCR components and conditions

Table 12. Reaction mix conditions to perform qrt-PCR, following manufacturer´s instructions.

Reagent	**[Final]**		**Volume from stock to prepare mix (µL)**
GoTaq Probe qPCR Master Mix (2X)	1X		10
GoScript RT Mix for 1-Step RT-qPCR (50X) (with CXR reference dye already mix at final concentration of 30nM)	1X		0,4
Primer Forward (18 µM)	900nM		1,0
Primer Reverse (18 µM)	900nM		1,0
Probe (5 µM)	250nM		1,0
RNA	40ng		3,0
Nuclease-Free Water	-		3,6
			Final volume: 20 µL
Run TaqMan Program in Applied 7500	**Temp**	**Time**	**Cycles**
Reverse transcription	45°C	15 min	1
Reverse transcriptase inactivation and GoTaq® DNA Polymerase activation	95°C	2 min	1
Denaturation	95°C	15 sec	40
Annealing and extension	60°C	1 min	

3.9.3 Generation of DNA standard for the qrt-PCR

The standard curve preparation was made following Applied Biosystems Manual. The sequence of the gBlock specific for ZIKV was amplified using the primers M13R/M13F (Table 6), with a size of 353bp, and then purified using the CELLCO Agarose Gel Extraction kit. The stock concentration of the gBlock was determined to be 18ng/µL by spectrophotometric analysis.

The PCR reactions were set-up such that 3µL of plasmid DNA were pipetted into each PCR reaction.

The copy of RNA (molecules/mL) was calculated as follows: Calculation of gBlock mass with "n" being 353pb: 353pb x $1{,}096 \times 10^{-21} = 3{,}868 \times 10^{-19}$g (Step 1)

$$m = \left[n \right] \left[1.096e\text{-}21 \ \frac{g}{bp} \right]$$

The formula above was derived as follows

$$m = \left[n \right] \left[\frac{1 \ mole}{6.023e23 \ molecules \ (bp)} \right] \left[\frac{660 \ g}{mole} \right] = \left[n \right] \left[\frac{1.096e\text{-}21 \ g}{bp} \right]$$

where:
n = DNA size (bp)
m = mass
Avogadros number = 6.023e23 molecules / 1 mole
Average MW of a double-stranded DNA molecule = 660 g/mole

Then, it was necessary to calculate the mass of gBlock containing the copy number of interest, which was between 300.000 to 30 copies (copy number of interest × mass of gBlock= mass of DNA needed). For example, mass of gBlock containing 300,000 copies ZIKV sequence is:

$$3{,}868 \times 10^{-19}\text{g} \times 300{,}000 \text{ copies} = 1{,}17 \times 10^{-13} \text{ g} \quad \text{(Step 2)}$$

The calculation of the concentrations of gBlock was made to achieve the copy numbers of interest, dividing the mass (calculated in Step 2) by the volume to be pipetted into each reaction. In this case, 3µL of gBlock solution was pipetted into each PCR reaction.

$$\text{For 300.000 copies: } 1{,}17 \times 10^{-13} \text{ g} / 3 \ \mu\text{L} = 3{,}9 \times 10^{-14} \text{ g/mL} \quad \text{(Step 3)}$$

Knowing the concentration of DNA needed for each point of the curve, serial dilutions of the gBlock were made. Since cloned sequences are highly concentrated in purified plasmid DNA stocks, a series of serial dilutions must be performed to achieve a working stock of DNA for quantitative PCR applications, which is $2x10^{-12}$ g/µL. In this case, two serial dilutions of 1:100 were prepared to achieve that concentration.

Once the DNA was in a workable concentration, $C_1V_1 = C_2V_2$ formula was used to calculate the volume needed to prepare the 300,000 copies standard dilution, then 1:10 serial dilutions were made until reach 30 copies, as shown on Table 13.

Table 13. Preparation of a serial dilutions of the gBlock of ZIKV for standard curve

Dilution	Source of DNA for dilution	[Initial] (g/µL)	DNA (µL)	Nuclease free water (µL)	Final vol (µL)	[Final] (g/µL)	Resulting copy number/ 3µL
1	Stock	$1,8x10^{-8}$	10	990	1000	$1,8x10^{-10}$	N/A
2	Dilution 1	$1,8x10^{-10}$	10	990	1000	$1,8x10^{-12}$	N/A
3	Dilution 2 (workable concentration)	**$1,8x10^{-12}$**	**2,7**	**97,83**	**1000**	$3,9x10^{-14}$	300.000
4	Dilution 3	$3,9x10^{-14}$	10	90	100	$3,9x10^{-15}$	30.000
5	Dilution 4	$3,9x10^{-15}$	10	90	100	$3,9x10^{-16}$	3.000
6	Dilution 5	$3,9x10^{-16}$	10	90	100	$3,9x10^{-17}$	300
7	Dilution 6	$3,9x10^{-17}$	10	90	100	$3,9x10^{-18}$	30

N/A: Not Applicable

Each dilution was loaded in triplicates. A water negative control (also run in triplicates) without gDNA, was used to rule out the possibility of primer dimers or gDNA contamination.

3.10 Study of the effect of ZIKV infection on cav-1 gene expression in THP-1 cells.

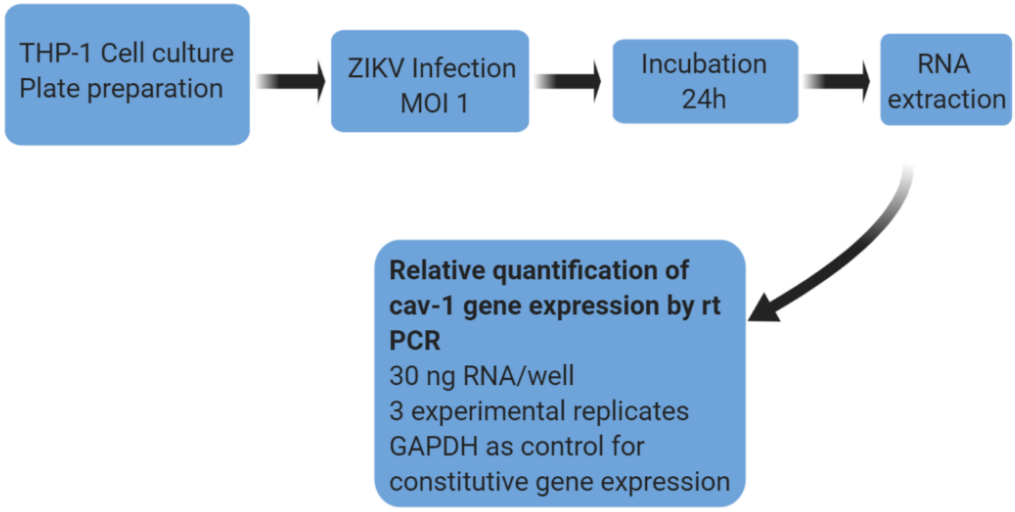

Figure 3. Role of ZIKV on cav-1 relative qrt-PCR

After evaluation of the effect of the depletion of lipid rafts on ZIKV replication, it was important to study if, inside lipid rafts, cav-1 protein was important on the context of ZIK infection (Fig. 3). In order to do that, THP-1 cells were infected with ZIKV with M.O.I.1, as described in section 3.5.

After 24 hours post infection, cells were collected to perform RNA extraction and evaluate levels of expression of cav-1 protein, comparing infected cells with control cells (not infected) through relative rt-PCR, as described below.

3.10.1 Relative quantification real time PCR

Levels of cav-1 gene expression was determined by real time-PCR using GoTaq® 1-Step RT-qPCR System (Promega) according to the manufacturer's instructions. Fluorescence detection was performed using SYBER Green I as fluorescence dye. The data were analyzed with Thermocycler 7500 real time PCR System (Applied Biosystems) and gene quantification was made using the $2^{-\Delta\Delta CT}$ method.

3.10.2 Primer design

Two sets of real-time primers for cav-1 mRNA were generated by IDT - Integrated DNA Technologies, Brazil. The sequence of the first set of primers (AR1) was taken from Wang *et al*. (2018). The second set (AR2) was design using the Primer-BLAST

tool of National Center for Biotechnology Information (NCBI), using gene bank access code NM_001753. Details for Primer sequences are shown in Table 6. All primers were confirmed using the MultiAline tool against the cav-1 mRNA sequence to ensure specificity.

A sequence of GAPDH mRNA was simultaneously amplified to serve as internal control, being the constitutive expressed gene, primers sequences are described in Table 6. At the end of each run, melting curve analysis was performed to ensure the specificity of the amplification. All samples were amplified in triplicates from the same RNA preparation.

3.10.3 Relative qrt-PCR components and conditions

Table 14. Reaction mix conditions to perform relative quantification of gene expression levels by qrt-PCR, adapted from manufacturer´s instructions.

Reagent	**[Final]**		**Volume from stock to prepare mix (µL)**
GoTaq qPCR Master Mix (2X)	1X		7,5
GoScript RT Mix for 1-Step RT-qPCR (50X)	1X		0,3
Primer Forward (10 µM)	200nM		0,3
Primer Reverse (10 µM)	200nM		0,3
RNA	30ng		3,0
Nuclease-Free Water	-		3,6
			Final volume: 15 µL
Run TaqMan Program in Applied 7500	**Temp.**	**Time**	**Cycles**
Reverse transcription	37°C	15 min	1
Reverse transcriptase inactivation and GoTaq® DNA Polymerase activation	95°C	10 min	1
Denaturation	95°C	10 sec	40
Annealing and data collection	60°C	30 sec	
Extension	72°C	30 sec	

3.11 Generation of vectors to change level of cav-1 protein expression on THP-1 cells.

To evaluate different expression levels of cav-1 in the context of ZIKV infection, several cloning systems were generated, either to increase or decrease cav-1 mRNA expression on THP-1 cells (Fig.4).

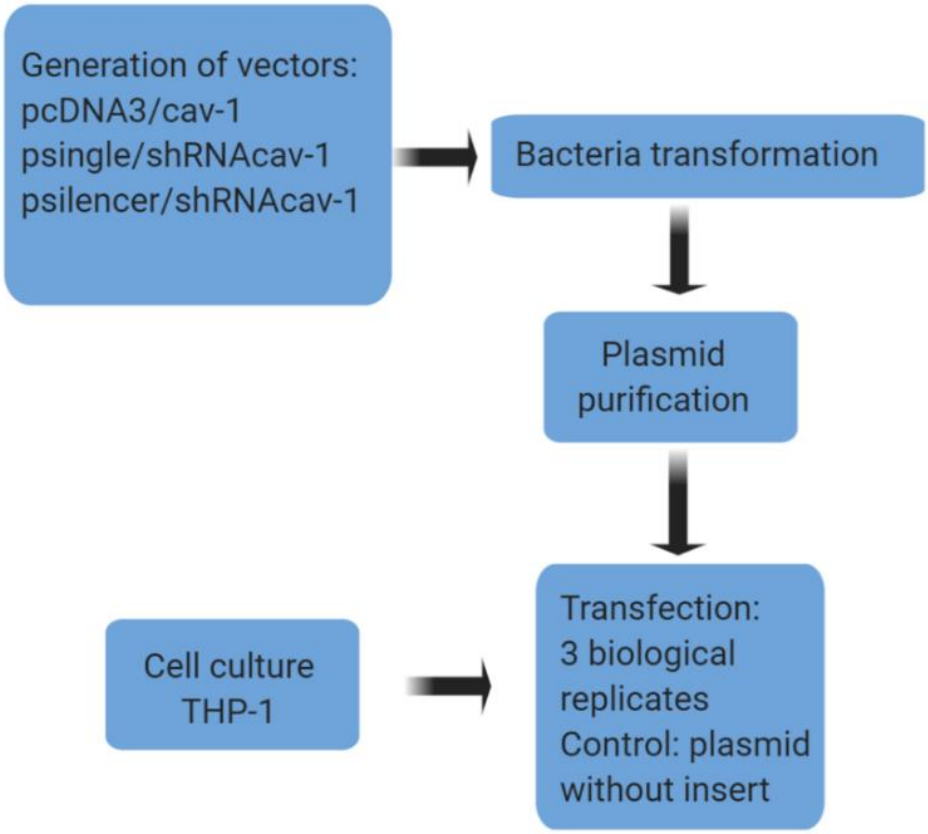

Figure 4. Generation of clone vectors to transfect human cells.

3.11.1 Processing of vector and insert

All plasmids used in this study were digested in separate solutions with their specific restriction enzymes, as described below.

Table 15. Reaction solution for plasmid digestion

Plasmid	DNA (ng)	Buffer R 10X (uL)	HINDIII (U)	BAMHI (U)	XhoI (U)	Free nuclease H_2O
pSingle-tTS-shRNA	400	1	10	-	10	Up to 10uL
pSilencer™ 3.1-H1 neo-shRNA	400	2	12	6	-	Up to 20uL
pcDNA™3.1(+) and gBlock-cav1 PCR product	400	1	6	3	-	Up to 10uL

For the silencing systems, each pair (shCAV1 for pSingle and caveolin-sh for pSilencer, described in Table 8) of single-stranded oligonucleotides with complementary sequences were annealed following KnockoutTM Single Vector User Manual (Section VI.B) and then used as inserts in the DNA ligation step.

For caveolin-1 super-expression system, the insert was amplified by PCR using CAV1-F and CAV1-R primers (Table 7), using the reaction mix and PCR program described in Table 16. Then, the PCR product was loaded into a 1,5% agarose gel run at 90V for 1 hour to confirm gBlock expected size, of approximately 0,6 kb. Then, the band of interest was excised from the gel and the DNA was extracted using an agarose purification kit (CELLCO), following the manufacturer's instructions.

The recovered DNA was digested, in parallel to the pcDNA™3.1 plasmid vector, as specified in Table 15.

Finally, both PCR insert, and digested vectors were loaded into a 1,5% and 1% agarose gel, respectively, and run at 90V for 1 hour. An undigested negative control for each vector was also run to assess complete digestion. Afterwards, the bands of interest were excised from the gel, and the DNA was extracted as described before. The concentration of the purified DNA were quantified by spectrophotometry, using NanoDrop Lite Spectrophotometer from Thermo Scientific.

Table 16. PCR for cav-1 gBlock insert processing.

Reagent	Amount for 1X		
10X buffer Mg^{2+} Plus	10µL		
dNTP mix (10µM)	2µL (200mM final concentration)		
Forward Primer CAV1-F (10µM)	2µL (200mM final concentration)		
Reverse Primer CAV1-R (10µM)	2µL (200mM final concentration)		
DNA TaqPol 500U	0,5µL		
Nuclease free H_2O	Up to 100 µL		
DNA template	1-10ng		
PROGRAM (Thermal Cycling Veriti 96 well Applied Biosystems)			
Preheated lit	95°C		
Initialization	95°C	5min	
Denaturation	95°C	30seg	30 cycles
Annealing	Tm – 5°C*	30seg	
Elongation	72°C	45seg**	
Final elongation	72°C	7 min	
Final hold	4° C	∞	

***Annealing temperature depends on the primer's Tm.**

**** TaqPol has a processivity of 0.9kb/min and the extension time was calculated according amplicon size.**

3.11.2 DNA binding reaction

To proceed with the ligation step, it was used a 1:3 molar ratio of pcDNA3 vector/cav-1 insert (the vector: insert ratio vary depending on their size). For this, 100ng of the plasmid and 32ng of the gBlock were mixed with water containing 10U of T4 ligase enzyme and 1X ligase buffer. The reaction was incubated for 3 hours at room temperature.

For both silencing systems, psingle and pSilencer, it was necessary to assemble two ligation reactions of each annealed ds-oligonucleotides for each plasmid, following KnockoutTM Single Vector User Manual (Section VI.C).

3.11.3 Preparation of XL-10 competent cells

In order to clone all three vectors, it was used *E. coli* XL10-Gold. This host bacteria was inoculated into medium A (LB broth supplemented with 10mM MgSO4 7H20 and 0.2% glucose, pH 7.0) and grown over-night under 180rpm shaking at 37°C (Incubator Shaker C24, EDISON, NJ USA) until reaching the mean log phase (A_{600} = 0.4).

Cells were kept on ice for 10 minutes and then centrifuged at 1500g at 4°C for 10 minutes. Finally, cells were carefully resuspended in ice cold medium A, combined with medium B (36% glycerol, 12% PEG-MW7500, 12 mM 7 MgSO4). Aliquots were stored at -80°C.

3.11.4 Transformation of bacteria

The solutions containing the corresponded vector (plasmid/insert) were placed on ice and 2µL were used to transform 100µL of competent cells with gentle mixing. Negative controls of plasmids without inserts were also used for each system.

The cells were incubated on ice for 30 minutes to allow the DNA to diffuse, subsequently heat shocked at 42˚C for 45 seconds and immediately placed again on ice for 2 minutes.

Then, 900µL of LB media without antibiotics were added to the heat-shocked cells, which were incubated for 1h at 37˚C (with gentle shaking) to allow their recovery. Passed this time, 100µL of transformed cells were seeded in the appropriate LB-antibiotic plates containing 5% w/v LB agar and 50 µg/mL of ampicillin, and incubated overnight for 18 hours at 37˚C.

3.11.5 Bacterial colony PCR

The colonies of transformed cells that grew in the selection media were collected from the Petri dishes and used as a template for the PCR reaction to verify the presence and size of the insert. The PCR reaction for the colonies containing the vectors is described on Table 16. Primer variations explained as follows:

Table 17. Evaluation of successfully transformed cells with each vector.

Vector	Primers	Amplicon size
pcDNA3/cav-1	Forward: T7 Reverse: BGH	Positive amplification product: **762pb** Negative amplification product: **186pb**
psingle/shRNAcav-1	Forward: ar3F Reverse: ar3R	Positive amplification product: **350pb** Negative amplification product: **no amplification product**
PSilencer/shRNAcav-1	Forward: MF13 Reverse: ar3R	Positive amplification product: **450pb** Negative amplification product: **385pb**

Finally, the PCR products were loaded into a 1,5% agarose gel to confirm the size of each insert, and run at 90V for 1 hour.

One of those colonies that amplified a product with the expected size for each system were picked to proceed with the plasmidial DNA extraction. Each single colony were inoculated in a starter culture of 5mL LB medium containing ampicillin (50 µg/ml) and incubated for 8h at 37°C with agitation.

3.11.6 Plasmid DNA preparation

All plasmid preparations were performed using MIDIPREP plasmid QIAGEN commercial kit and prepared according to the manufacturer's instructions.

First, 25mL of bacterial culture were inoculated with 25µL of the starter culture for each vector and then grown overnight at 37˚C and shaking. Second, the bacterial cells were harvested by centrifugation. Third, the bacterial pellet was re-suspended in RNAse A containing buffer and lysed under alkaline conditions (pH 12) given by the presence of NaOH in the lysis buffer. Alkaline lysis allowed denaturation of chromosomal DNA and proteins while plasmid DNA remained stable. Successful lysis could be noticed by the color change of the pH indicator (if contained in the buffers) or by the suspension's change of consistency and appearance of mucus, corresponding to the chromosomal DNA, intracellular proteins and solutes.

Subsequently, the lysate was neutralized upon addition of acetate-containing buffer, which further precipitated large chromosomal DNA and proteins while plasmid DNA remained soluble. Once all intracellular molecules, except for the plasmid DNA, where denatured and precipitated, plasmid DNA was purified using spin-columns, whose solid matrix bound to the negatively charged DNA and allowed other components to flow through. Plasmid DNA were eluted upon changing the charge conditions of the column.

Finally, the eluted DNA was precipitated with isopropanol and ethanol to allow further concentration, air dried and redissolved in TE buffer pH8.0. The concentrations of each plasmid purification were measured using NanoDrop Lite Spectrophotometer, and the plasmids were either used or stored at -20˚C. Electrophoresis was performed to confirm good quality plasmid purification.

3.12 Evaluation of the effect of the levels of cav-1 gene expression on ZIKV infection in THP-1 cells

After successful generation of cloning systems carrying vectors to transfect THP-1 cells, ZIKV viral replication was quantified on each condition by qrt-PCR and plaque assay (Fig. 5).

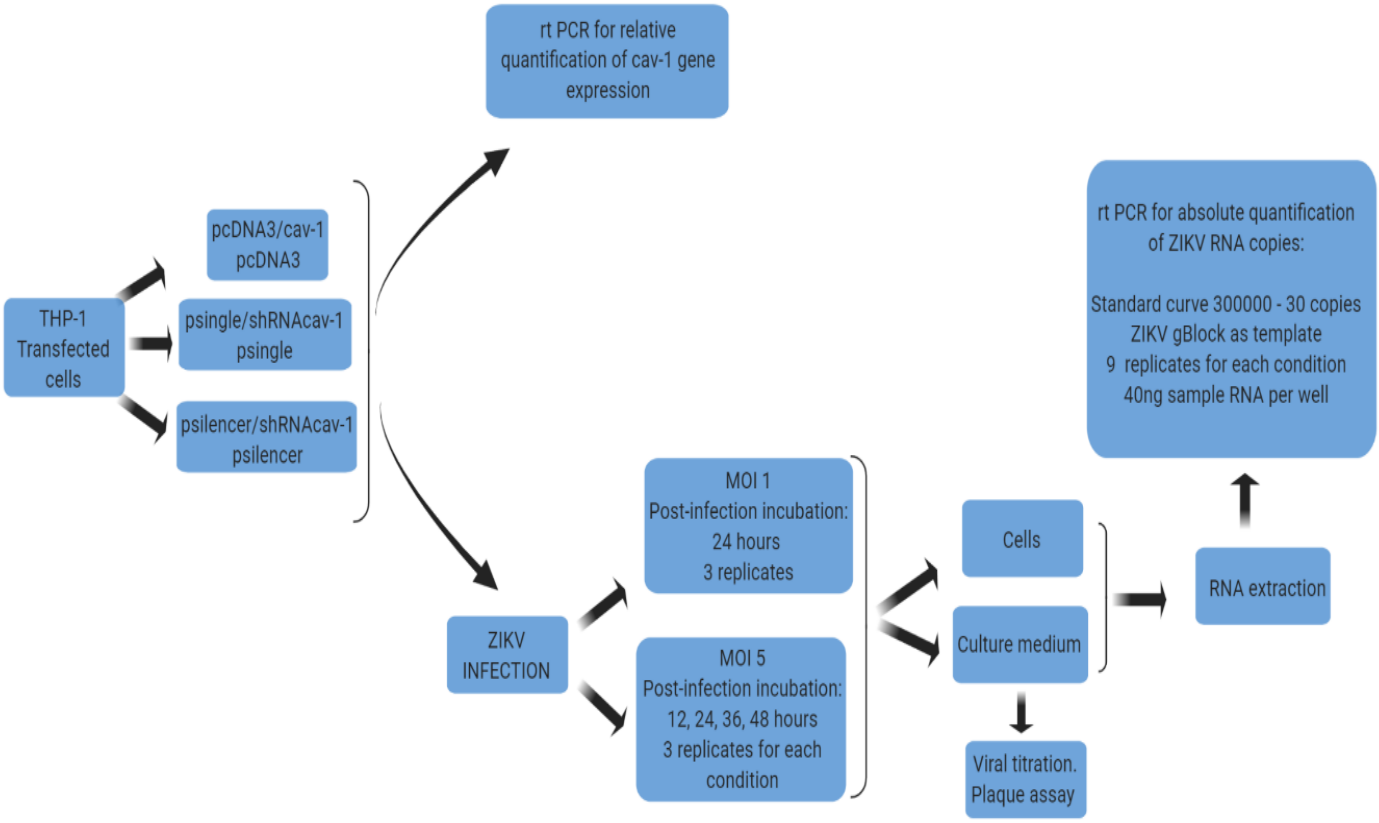

Figure 5. Evaluation of different expression levels of cav-1 in the context of ZIKV infection

3.12.1 Transient Transfection of THP-1 cells.

All purified plasmid DNA were treated with Lipofectamine 3000 Transfection Reagent, as described by the supplier, and mixed with the cell suspension. To analyze if transformation succeeded, cell samples were collected and their RNA were isolated to perform a relative qrt-PCR in order to evaluate cav-1 expression, as described in section 3.10.1. Control cells were used, transfected with plasmid vector without the insert.

In order to do that, 24 hours before transfection 24- well plates were seeded at a cell concentration of approximately $2x10^5$ cells per well. After the incubation time

at standard conditions, THP-1 cells were transfected with the lipid transfection reagent Lipofectamine 3000 that forms Lipid-DNA complexes upon mixing with DNA, which is capable of penetrating the plasma membrane while delivering DNA to recipient cells.

The transfection was performed using, for each well, 0.75µl of Lipofectamine Reagent diluted in 25µl Opti-MEM Reduced Serum Medium. Then, the master mix of DNA was prepared diluting 500ng of plasmid DNA in 25µl of Opti-MEM medium and adding 2 µl of P3000 reagent. This solution was mixed with the diluted Lipofectamin Reagent in a 1:1 ratio and then incubated for 15 min at room temperature. Finally, 50 µl of the Lipid-DNA complex was added to the cells.

Cells were incubated 48 hours in standard conditions, before analyzed for transfection efficiency with rtPCR and continue with further experiments.

Since psingle/shRNAcav-1 contains a tetracyline-controlled transcriptional suppressor, it has a tetracycline-inducible expression. To achieve an efficient depletion of the gene of interest, transfected THP-1 cells were incubated with 1µg/mL of tetracyline for 2h and then analyzed for silencing efficiency. Later on, concentrations of 1, 5 and 10 µg/mL were tested with incubations times of 2, 6, 18 and 24 hours to evaluate which condition was best for gene silencing, using rtPCR.

3.12.2 Infection of transfected cells with ZIKV

Effectively transfected THP-1 cells were infected as described in section 3.5, with M.O.I.1 and 5 and incubated for 24 hours post-infection. Past this incubation time, cells were collected for RNA purification (section 3.8) to study viral load inside the cell using qrt-PCR (section 3.9), and the culture medium was harvested to evaluate viral titration through plaque assay (section 3.7).

For M.O.I.5, culture medium was harvested every 12 hours until 48 hours of post infection time were completed. Simultaneously, for M.O.I.1 culture medium was collected only at 24 hours post infection. Virus samples were tittered by plaque assay.

3.13 Statistical Analyses

Statistical comparisons were performed using unpaired Student's t-test, one-way and two-way ANOVA (post-hoc Tukey and Sidak's multiple comparisons test, respectively) and Mann-Whitney test (with Bonferroni correction) as indicated. All tests were carried out using GraphPad Prism version 7.0 software. A P value < 0.05 was considered significant. The means and standard deviation are shown in all graphs. For the details of each analysis on each experiment, see Appendix 9.6.

4 Results and discussion

4.1 Methyl β-cyclodextrin cytotoxicity assay

Numerous studies have shown that exposing cells to MβCDs results in removal of cellular cholesterol (BARMAN & NAYAK, 2007; DOU et al., 2018; SUN & WHITTAKER, 2003), and variations in methodology suggests that the degree of cholesterol depletion can vary according to the used concentration, incubation time, temperature and type of cells.

It has been reported that when cells are exposed to high concentration of MβCD (5–10mM) for a prolong period of time (>2 hours) 80–90% of total cellular cholesterol can be removed (KILSDONK et al., 1995; LEVITAN et al., 2000). Nevertheless, under these conditions, cells typically lose their morphology and in extreme cases become non-viable.

Based on those observations, it became clear the importance of verifying the effect of MβCD on the experimental conditions of this study, thus in order to determine whether MβCD treatment for membrane cholesterol depletion on THP-1 cells had a negative influence on cell viability, several concentrations were tested as described in section 3.4.

The range of tested concentrations were picked following the literature suggestions where Zidovetzki and Levitan (2007) reported that relatively high (≥10mM) MβCD concentrations and relatively long (≥ 30 min) exposures will lead to cholesterol depletion from all membrane fractions. And (GAUS et al., 2005) proved that with 10mM of MβCD for 1h of incubation ~85% of cholesterol depletion was achieved in THP-1 cells.

As shown in Fig.6 (A) only at a concentration of 5mM, treated cells maintained the same number of viable cells as control cells, higher concentrations showed detrimental effects on cell viability, after 1 hour of treatment. Effects of MβCD treatment on cellular cholesterol level are indirectly measurable for its presence on culture medium. As shown in Fig. 6 (B), it was observed that, with increasing concentrations of MβCD, more cholesterol was found on culture medium.

Even when there is no significant differences between the cholesterol concentration on culture medium of control cells and culture medium of cells treated with 5 and 10mM MβCD, it is noticeable that cholesterol was present in the media, on the contraire of the control condition where measurements were null.

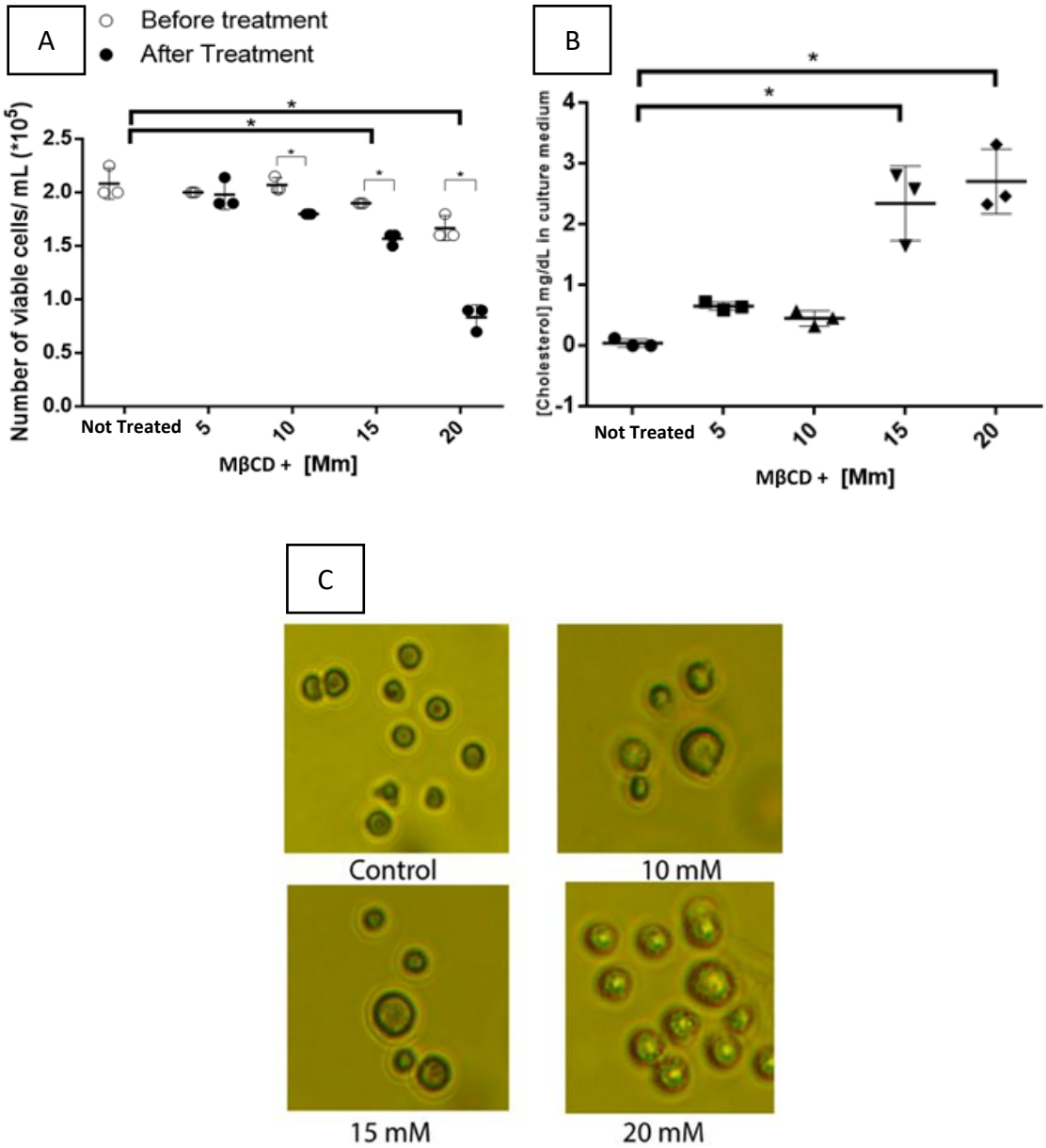

Figure 6. Cytotoxicity of MβCD treatment on THP-1 cells. (A) Viable number of cells after several concentrations of MβCD treatment, significant cytotoxicity was only seen at 20mM. *p 0.05 (KW-1-way ANOVA). **(B)** Effects of MβCD treatment on cellular cholesterol levelSeeing that in the context of cell viability the concentration of 5mM MβCD was less aggressive on cells than the concentration of 10mM and the cholesterol concentration found in the culture medium of both conditions were similar, the 5mM MβCD concentration was used for all subsequent experiments. *p 0.05 (2-way ANOVA). **(C)** Morphology changes on THP-1 cells in each condition (5 and 10mM are represented by the same image, since both conditions presented similar morphology)

4.2 ZIKV infection in cells treated with MβCD

Some proteins are concentrated within lipid rafts, which are cholesterol-rich assemblies on the plasma membrane. Among those proteins, there is cav-1 protein (CORDERO et al., 2014). Since depletion of cholesterol affect the assembly of proteins complex associated with lipid rafts, evaluation of the level of expression of cav-1 mRNA after treatment with MβCD on both, infected or not infected cells with ZIKV, was performed.

The results on Fig. 7 (A) showed that, even though it can be observed a slight increase in cav-1 levels on infected and treated cells, it has no significant difference compared with non-infected cells. It was next observed the effects of MβCD treatment on the production of intracellular ZIKV RNA on infected THP-1 cells. The results showed that cells lacking cholesterol on cell membranes lowers the production of ZIKV, as shown in Fig. 7 (B), suggesting that cholesterol content in cell membrane is important in the ZIKV replication cycle.

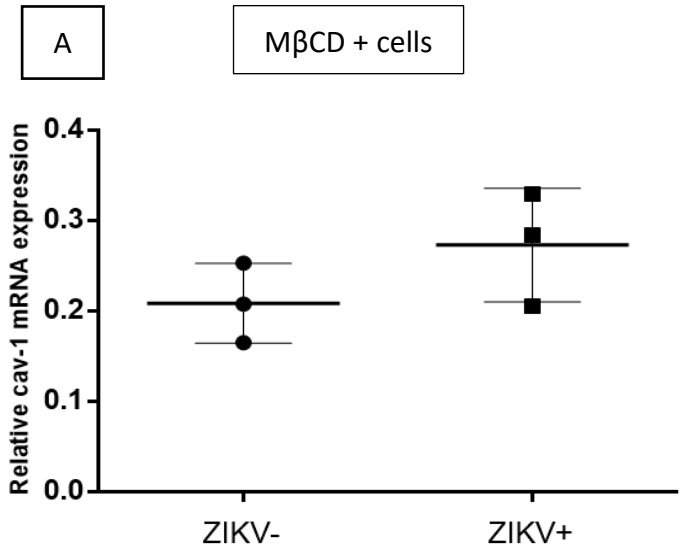

Figure 7. Evaluation of ZIKV infection (MOI. 1, 24h post-infection) on THP-1 cells treated with MβCD (5mM, 1h incubation). **(A)** Comparison of expression levels of RNAm cav-1 on MβCD treated cells, infected or not with ZIKV. No significant difference was observed.

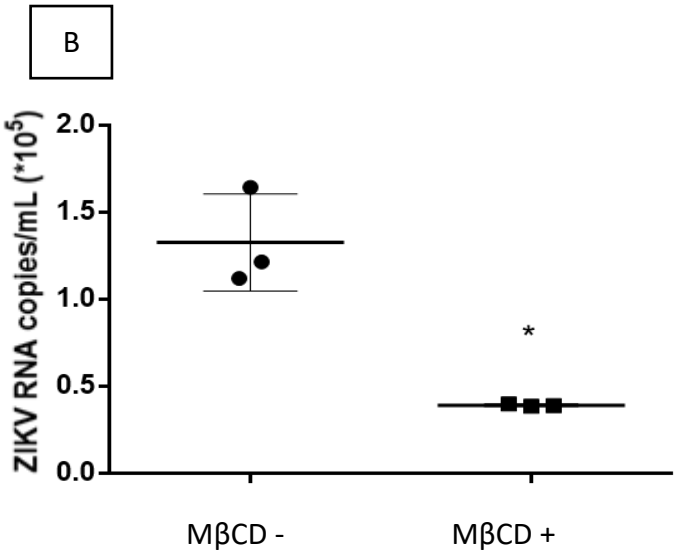

Figure 7. (B) Comparison of ZIKV RNA levels between not treated and treated cells. ZIKV RNA copies was significantly reduced upon MβCD treatment. *p 0.05 (Student's t-test)

Numerous studies have shown that cholesterol depletion results in disassociation of a variety of proteins from detergent resistant/low-density membrane fractions (where membrane rafts are located) (PREDESCU et al., 2005; SHEETS et al., 1999). Furthermore, cholesterol depletion induces significant changes in the physical properties of these fractions, as revealed by measuring diffusion of raft-associated proteins (PRALLE et al., 2000).

Additionally, it is known the non-specific effects of MβCD on cell membranes, as it has been shown that it may interact with membrane phospholipids and membrane proteins, hence cholesterol depletion can also result in disappearance of caveolae as stated by (DREJA et al., 2002).

It has also being reported that the cholesterol requirement during virus replication is high (OSUNA-RAMOS et al., 2018). Thus, when cholesterol content in cell is low, in this case due to depletion with MβCD, viruses directly manipulate the host cell pathways involved in the uptake and biosynthesis of cholesterol to increase the levels, as already described for flaviviruses WNV (MACKENZIE et al., 2007) and DENV (MARTÍN-ACEBES et al., 2016).

Infection with WNV causes redistribution of cholesterol from the plasma membrane to the sites of replication (ESPAÑO et al., 2019). Lipid rafts are hypothesized to be involved at this stage in order to increase the surface area available for viral replication and to concentrate the replication factors within the vesicle packets (MARTÍN-ACEBES et al., 2016).

Viral replication is a complex process that involves many host factors including lipid metabolism and rearrangement (STAPLEFORD & MILLER, 2010).

Viruses interact with host lipids to enhance replication, however this depends on the type of Flavivirus, for example WNV requires cholesterol-rich micro-domains to entry the cell (MEDIGESHI et al., 2008), whereas DENV and JEV entry is meaningfully blocked by cholesterol enrichment (LEE et al., 2008a), suggesting a preferential requirement of lipids between viruses within the same family.

Furthermore, all (+)RNA viruses, including ZIKV depend on lipids to induce viral complexes that are vital for efficient viral replication (MARTÍN-ACEBES et al., 2011).

Flaviviruses have evolved to exploit lipid rafts to establish infection by modulating several molecules that are gathered in those micro-domains to mediate entry into cells, for example JEV and WNV both require lipid enriched membrane-platforms to enter and egress from cells, respectively (AKTEPE & MACKENZIE, 2018).

Authors like (TANI et al., 2010) showed that the increase in membrane-bound ceramide (a type of lipid present in cell membrane) by sphingomyelinase treatment significantly increased JEV infection, whereas reduction in ceramide levels had opposing effects.

In addition, it was found in (DAS et al., 2010) that disruption of lipid raft formation by cholesterol depletion using MβCD reduced JEV RNA levels and production of infectious virus particles. Similarly in WNV, sequestration of cholesterol from the plasma membrane resulted in lower viral titers and failed virus internalization (STIASNY et al., 2003), such as the results found on this study for ZIKV. These observations suggested that in some flaviviruses, cholesterol influences early stages of infection.

In contrast, another study in DENV demonstrated that disrupting cholesterol biosynthesis did not inhibit replication but resulted in lower virus production, indicating a role for cholesterol in later stages of viral biogenesis (PEÑA & HARRIS, 2012). As result, several studies have been performed to identify the stages in flaviviral replication cycle where cholesterol is involved.

Indeed, DENV and JEV replication has been shown to occur in cholesterol microdomains or lipid rafts inside the cell (LEE et al., 2008a). Nevertheless, lipid rafts are not only important for virus entry, but for viral translation and replication. For example, it was found that DENV alters cellular membrane structures, upon infection. Therefore, it is possible that its replication complex is recruited to lipid rafts structures, which then provide a platform for RNA replication in cellular membranes, as has been observed for the hepatitis C virus (SHI et al., 2003).

All of these factors raised the question of which components of lipid rafts, other than cholesterol could be affecting replication cycle of ZIKV. One important protein that is part of lipid rafts present in cell membranes, cav-1, is also involved in several signaling pathways used for flaviviral replication cycle. Therefore, evaluation of expression levels of this protein upon infection was made.

4.3 Study of cav-1 upon ZIKV infection in THP-1 cells.

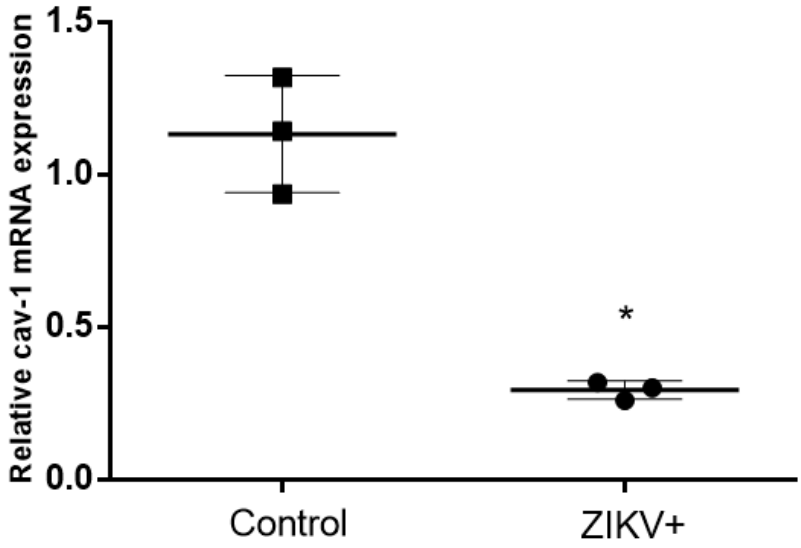

Figure 8. Comparison of levels of expression of cav-1 mRNA on THP-1 infected or not with ZIKV (MOI. 1, 24h post-infection). *p 0.05 (Student's t-test).

Results showed that there is a significant decrease in cav-1 mRNA expression in THP-1 infected cells compared with non-infected cells (Fig.8).

The cav-1 protein plays a major role in the regulation of cell differentiation, proliferation, migration, apoptosis, and other important functions of the cells (DIAZ-VALDIVIA et al., 2015), therefore it is clear that is involved in many cell signal pathways.

It is known that viruses often hijack host cellular signaling pathways to facilitate their infection and replication. Several pathways, such as the MAPK, PKA, and AMPK pathways, have been reported to play important roles in flavivirus replication (FAN et al., 2018) and it has been described that cav-1 inhibits the MAPK pathway (GONZALEZ et al., 2004; YIN et al., 2016). The main members of the MAPK family are JNK and ERK, and caveolin-1 can inhibit ERK activation through many ways, such as by blocking the downstream transmission of signals (FIUCCI et al., 2002).

A number of inflammatory signaling pathways such as ERK, p38MAPK, NF-κB, JAK/STAT3 and endoplasmic reticulum stress are activated after ZIKV infection (AHN et al., 2017), therefore ZIKV could contribute to the decrease on cav-1 expression in THP-1 to prevent inhibition of the inflammatory signaling pathways.

On the other hand, SHAH et al., 2002 described that IL-6/raft/STAT3 signaling is a pathway that involves cav-1 as accessory protein, in hepatic cells, that contributes to signaling maintenance during fever. Fever is a common response of the body to infection and injury and IL-6 is a major systemic mediator of this “acute-phase” response.

Nevertheless high levels of IL-6 are found after ZIKV infection (BAYLESS et al., 2016), therefore if the decreased levels of cav-1 on THP-1 found on this study is indeed consequence of ZIKV infection and are constant for other cells, like hepatic cells, then IL-6 response could be exacerbated through another pathway different than IL-6/raft/STAT3 signaling. Further studies need to be made on this matter.

Under this scenario, remained the question of if reduced levels of cav-1 protein were important for ZIKV replication or if on the contrary, high levels of the protein were unfavorable for the virus life cycle. Hence, the evaluation of the effect of the levels of cav-1 expression on ZIKV infection in THP-1 cells was made.

4.4 Knockdown of shRNA of cav-1 on THP-1 cells.

4.5 cav-1 knockdown using pSingle/shRNAcav-1 construct.

After completing the construction of the vectors (see appendix on section 9), THP-1 cells were transfected with each system.

For the first set of experiments, it was used psingle/shRNAcav-1 vector to determine whether a silencing effect could be achieved. It was decided to use a tetracycline-inducible depletion because, in that way, the silencing could be controlled in a time specific manner.

At first, it was used a single concentration of Tet at 1µg/mL and a single incubation time of 24h, then cells were analyzed at different times after transfection with different Tet concentrations; this was made with the intention of identifying possible differences in silencing events or efficiencies over time.

Results are depicted in figures below.

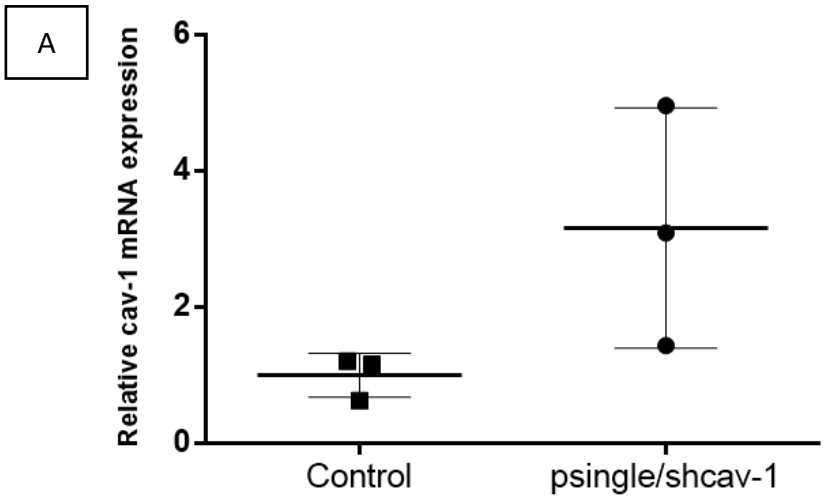

Figure 9. Evaluation of psingle/shRNAcav-1 effect after induction of transfected THP-1 cells. Control cells were transfected cells with an empty plasmid (without the target sequence for silencing). **(A)** Relative quantification of expression levels of cav-1 mRNA of cells collected after 24h of incubation with 1µg/mL of Tet. No difference found (Student's t-test).

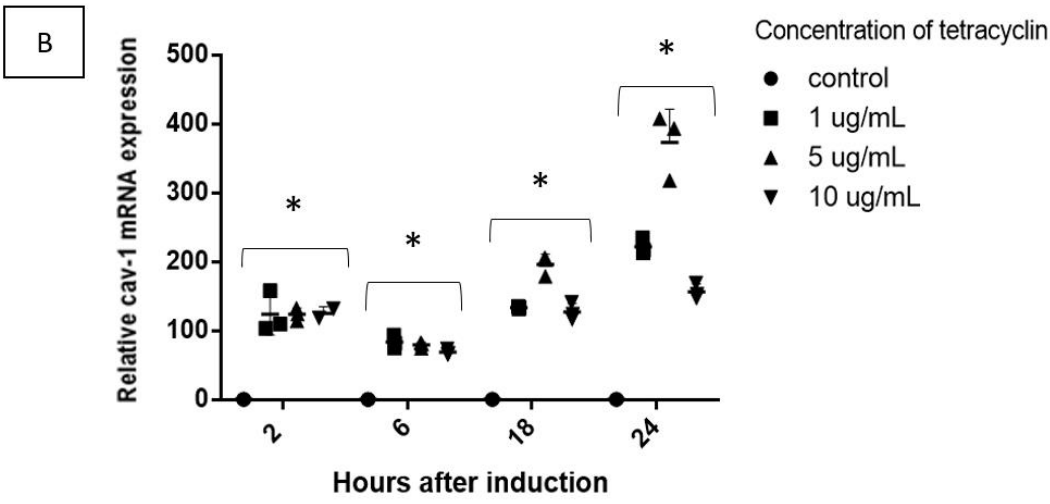

Figure 9. (B) Relative quantification of expression levels of cav-1 mRNA of cells collected after 2, 6, 18 and 24h of incubation with 1, 5 and 10 µg/mL of Tet. *p 0.05: Both variables, concentration of inductor and time of incubation, have an effect on cav-1 mRNA expression levels when compared with their own group control (2-way ANOVA).

Analysis of shRNA-transfected THP-1 cells did not show any silencing effects at any condition, instead, it was observed an overexpression of the cav-1 mRNA when compared with the control cells as shown in Fig. 9. The same effect persisted at the different tested incubation times and concentrations of treatment.

Further experiments to test more conditions to standardize cav-1 knockdown using tetracycline-inducible psingle-tTs-shRNA vector needed to be made, for example, studies like (GOMEZ-MARTINEZ et al., 2013) recommended to test clones expressing shRNA only 96h after Tet addition, placing more Tet every 24h to maintain the induction. Unfortunately, this was not a considerable option due to a lack of time limiting this project.

The creation of a stable shRNA cell line is a time-consuming task as the construct preparation and the selection of shRNA-positive cells by drug resistance or fluorescent markers may take months. Many cells cannot be transfected with shRNA at high levels (which is an important factor to take into consideration and also need to be standardized), especially primary and non-adherent cells, such as monocytes cells, used in this study.

The successful generation and application of inducible Tet cell lines is critically dependent on several factors. There are reports describing (HOHENWARTER, 2017; SANDY; VENTURA; JACKS, 2005; WENG et al., 2017) that gene knockdown attempts, using this system, also failed to induce silencing on several target genes.

Notably, previous reports suggested that the efficacy of silencing is affected by the accessibility of the target sequence and many other factors. Therefore, it is recommended to evaluate several methods to circumvent the present limitations of this technique. For example, earlier studies have done a screening of several sequences for the same target gene in their cell model, and have standardized conditions for an efficient delivery system (WENG et al., 2017).

CHO et al., 2009 and SCHERER et al., 2004 did a search for the optimum shRNA construct and demonstrated that some shRNAs have 'off-target' effects, such as interfering with the expression or function of other genes or proteins. This could explain the overexpression seen in this study, where the designed shRNA could have affected other proteins in the signaling pathway of cav-1 that resulted in higher levels of expression compared with the control cells.

BERNS et al., 2004 showed it is possible to overcome those off target effects by introducing, simultaneously into the cells, several different sequence fragments of a target gene, which results in an enhanced silencing efficiency when attempting to inhibit the function of a single gene.

Also, XING et al., 2008 used two shRNA interference vectors to silence one gene, and it was demonstrated that this method had better silencing effects than when a single shRNA vector was used. Lastly, HEALE et al., 2005 reported that secondary structure predictions of the mRNA may further improve si/shRNA design. Beyond off-target effects, it remains difficult to identify possible efficient sequences of shRNAs from among hundreds or thousands of prospects within a given transcript. Consequently, many shRNAs are ineffective (FELLMANN et al., 2011).

The exact sequence requirements of efficient RNA knockdown remain not fully understood, impeding the establishment of shRNA prediction rules. Studies using siRNA data sets (AMERES et al., 2007 and SCHWARZ et al., 2003) indicate that

sequence features in both the mature small RNA and the targeted mRNA region dictate RISC loading and target repression.

These include a preference for thermodynamic asymmetry (KHVOROVA et al., 2003), low G/C content and a strong bias for A/U at the 5´ end of the guide strand (REYNOLDS et al., 2004). Nonetheless, these features are not enough to differentiate, in a precise way, between potent and weak RNAi triggers.

Machine-learning-based applications trained on siRNA data sets have produced algorithms that facilitate prediction of potent siRNAs. However, such analyses do not apply to shRNAs, which may require more stringent criteria as they rely on transcription and multistep miRNA processing for the production of small RNA duplexes (VERT et al., 2006).

In addition, there is growing evidence that small RNAs can also serve as activators ofgene expression by targeting gene regulatory sequences; this could be another explanation for the results observed in Fig. 9.

This new discovered mechanism is known as RNA activation (RNAa) and seems to be conserved in mammalian cells, activated by both endogenous and artificially designed small RNAs. RNAa are linked to epigenetic changes and may support transcriptional activation of target genes, however the underlying mechanism remains poorly understood (PORTNOY et al., 2011).

Other studies (GONZALEZ et al., 2004) preferred to use variations of plasmid-based RNA interference techniques because their preliminary experiments showed that inducible-plasmid based methods had an unacceptably low transfection efficiency in their experimental model.

On this study it was used a plasmid with constitutive expression as an alternative for silencing.

4.6 Study of cav-1 knockdown using pSilencer/shRNAcav-1 construct in the context of ZIKV infection.

Even though constitutively silencing can be ubiquitously active, this type of gene silencing would not result in lethality of the cell and the amount of variables present for achieving silencing would be fewer, when comparing with the standardization that had to be made for psingle-tTs-shRNA system, where an transcription inductor had to be used.

As shown in Fig. 10(A) the transfection made with the pSilencer/shRNAcav-1 construct had a significant silencing effect on the level of mRNA expression of cav-1 when compared with control cells transfected with an empty plasmid. It was also observed a decrease in cav-1 mRNA levels in infected cells when compared with control. Nevertheless, the robust effectiveness that was expected for this study was not achieved, since expression levels of cav-1 mRNA were still maintained.

This outcome implies that, indeed, low levels of cav-1 may be favorable for ZIKV replication, supporting the hypothesis that arose of the results in Fig. 8, where it was thought that ZIKV infection was decreasing the levels of cav-1 in THP-1 cells as result of viral molecular hijacking to improve viral multiplication.

However when transfected cells with pSilencer/shRNAcav-1 were infected, levels of cav-1 increased with no significant difference when compared with infected cells transfected with pSilencer only; showing a lack of consistency in the results, that may be due to incomplete knockdown of cav-1.

Besides the low knockdown efficiency on THP-1 cells after transfection found in this study compared with the reported by (JAIN et al., 2010; WANG et al., 2013) with results of up to 95% of silencing, reproducibility inside the replicates on the same experiments turned out to be a major issue.

In many cases, the replicates were barely comparable to each other due to significant fluctuations of fluorescence detection when the number of ZIKV RNA copies were quantified by rt-PCR, as observed in Fig. 10 (B). In some conditions there was no detection at all, like is shown at 48h and at the same group of replicates at 24 and 36h.

Even when statistical analysis showed no difference between control and treatment for each evaluated incubation time, this is still to be yet confirmed due to the poor quality results obtained on this data set.

Finally, a titration assay with the culture media of infected cells was performed and no difference was found between conditions when compared to control as it may be noticed at Fig. 10 (C), indicating that decrease levels of cav-1 mRNA in THP-1 cells has no effect on the production of viable infecting viral particles.

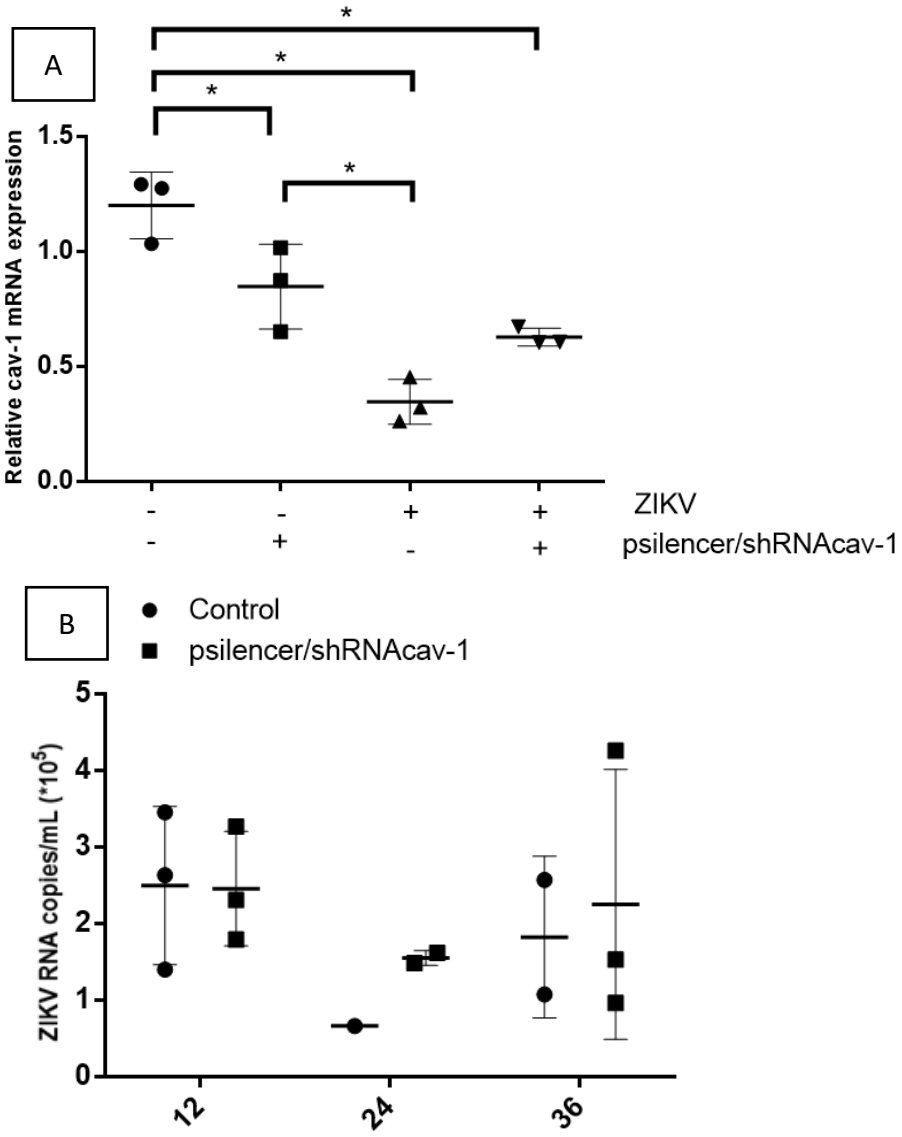

Figure 10. Study of pSilencer/shRNAcav-1 silencing effect on 24 hours infection at M.O.I of 5 using THP-1 transfected cells. (A) Comparison of cav-1 mRNA expression levels between cells transfected for 48h with pSilencer (designated as "–" for the presence of the insert) or pSilencer/shRNAcav-1 (designated as "+" for the presence of the insert), infected or not with ZIKV.*p 0.05 (one-way ANOVA). **(B)** Absolute quantification of ZIKV number of mRNA copies in pSilencer (control) transfected cells compared with pSilencer/shRNAcav-1 transfected cells, infected at MOI: 5 and collected after 12, 24, 36 and 48h of post infection time. No difference found (2-way ANOVA).

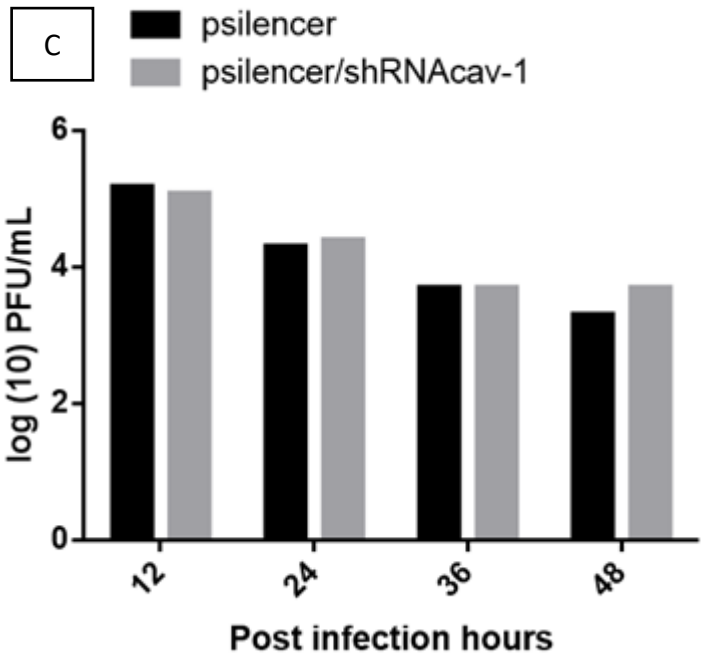

Figure 10. (C) ZIKV titration using plaque assay. Culture media of cells infected at a MOI: 5 were collected after 12, 24, 36 and 48h of post infection time to determine the Plaque Forming Units (PFU) per mL.

Transfection efficiency is a major issue for shRNA since incomplete transfection produces incomplete knockdown which may fail to ablate the function of the protein (CHRIS B. MOORE, et al., 2010).

Therefore, with reasonable levels of cav-1 still being express inside the cell, the evaluation of any impact on ZIKV replication cycle due to the lack of this protein becomes challenging since a vigorous silencing results are necessary to generate reproducible and representative results.

In an attempt to further discover a possible experimental error, it was decided to repeat the assay with only one incubation time of 24 hours, comparing viral load of M.O.I.1 and M.O.I.5, increasing the number of replicates to 12 per condition for ZIKV RNA quantification. The results are shown in Fig. 11.

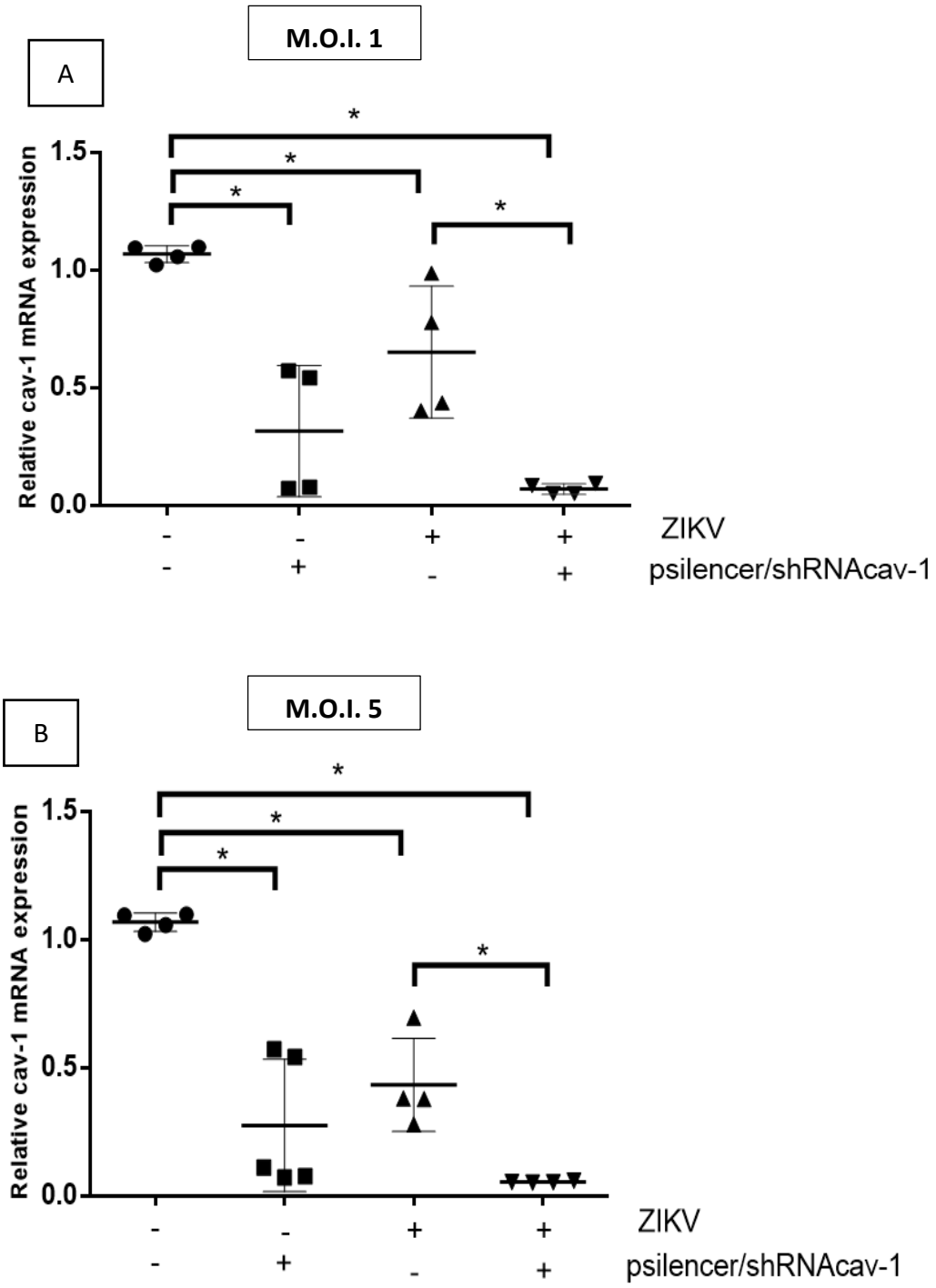

Figure 11. **Study of pSilencer/shRNAcav-1 silencing effect on 24 hours infection with ZIKV using THP-1 transfected cells.** Control cells were transfected with an empty plasmid (without the target sequence for silencing). **(A)** Comparison of cav-1 mRNA expression levels between cells transfected for 48h with pSilencer (designated as "–" for the presence of the insert) or pSilencer/shRNAcav-1 (designated as "+" for the presence of the insert), infected or not at MOI: 1, collected after 24h of post Infection time. *p 0.05 (one-way ANOVA). **(B)** Same conditions than A, with the difference of an increase viral load, at MOI: 5. *p 0.05 (one-way ANOVA).

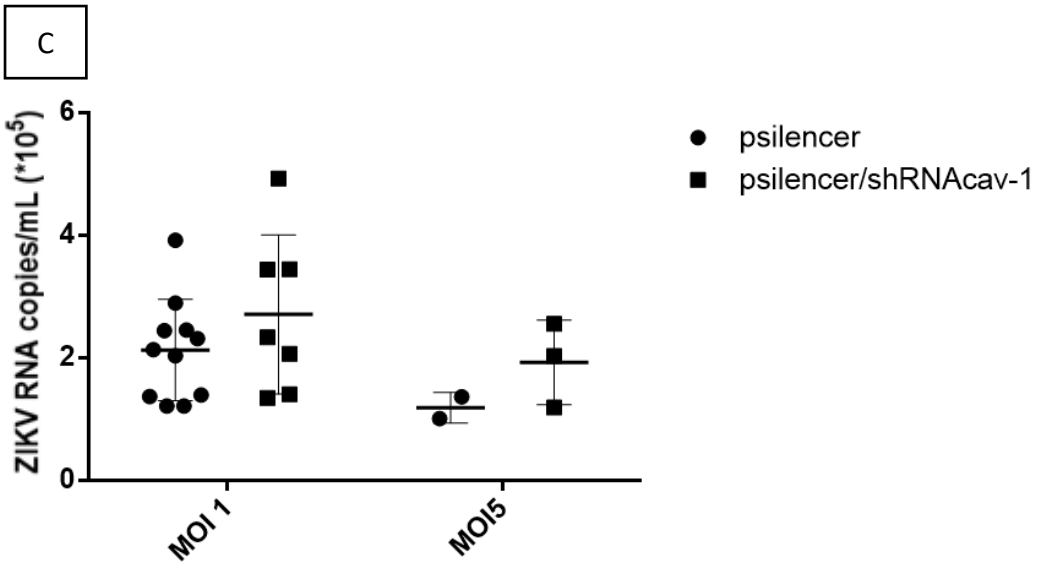

Figure 11. (C) Absolute quantification of ZIKV number of mRNA copies in pSilencer (control) transfected cells compared with pSilencer/shRNAcav-1 transfected cells, infected at MOI: 1 and MOI: 5 and collected after 24h of post infection time. No difference found (2-way ANOVA).

When comparing Fig.11 (A) and (B) with Fig.10 it can be noticed that a certain pattern is maintained, where a decreased of cav-1 mRNA levels is always achieved either by cav-1 silencing with transfection or by ZIKV infection.

Nevertheless, the inconsistency in the results persists. In this experiment, on both conditions of M.O.I.1 and M.O.I.5 (Fig. 11 A and B), there is a significant difference between not silenced and silenced cells infected with ZIKV, observing a complete knockdown of cav-1 mRNA in the condition of both infected and cav-1 silenced cells; which was not seen in the results shown in Fig. 10.

This time, detection for ZIKV number of RNA copies using qrt-PCR was achieved with a better performance, yet with detection limitations for M.O.I.5, where only few replicates showed strong fluorescence signals, as observed in Fig.11 (C). The result showed no difference between control and cells with decrease on cav-1 levels for intracellular ZIKV RNA quantification, reinforcing the primarily results shown in Fig.10 (D).

The variations in the results may be due to the technical detection limit that range between 5-10 copies/reaction. RNA purification methods could be optimized to obtain RNA viral stock concentrations with higher yield of what was obtain on these set of experiments (around 6ng/uL per condition).

In order to test the importance of RNA quality on the experiments, one last experiment was made with a better quality and quantity of purified RNA. The results showed an accumulation of ZIKV genome in the silenced cells (Fig. 12), to our knowledge this would be the first reported result for cav-1 affecting ZIKV multiplication.

Therefore, it becomes clear that it is necessary to standardize the transfection process in order to obtain a complete knockdown of cav-1 inside the cells and achieve reproducible results to continue the study of its possible effect on ZIKV replication. One possible viable way to improve the yield of future experiments would be changing the cell model to be adherent cells, where the role of lipid rafts is also important, since suspension cells have inherent properties that makes procedures very laborious in which loss of important material is generally unavoidable.

On this study, even when a decrease on the levels of cav-1 was always achieved, the results regarding its effects on ZIKV multiplication cannot be decisive due to the variations of the silencing effects for each experiment.

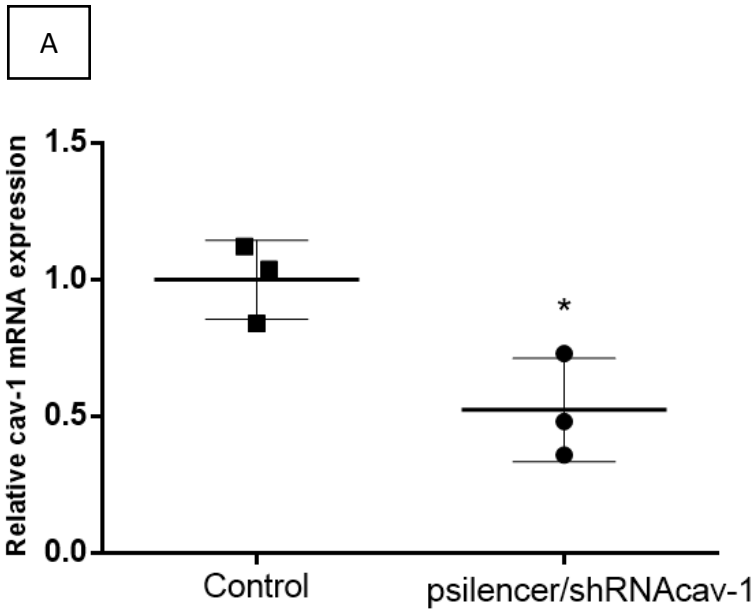

Figure 12. Evaluation of pSilencer/shRNAcav-1 silencing effect on infection with ZIKV using THP-1 transfected cells. Control cells were transfected with an empty plasmid (without the target sequence for silencing). **(A)** Relative quantification of expression levels of cav-1 mRNA of control cells compared with shRNAcav-1 transfected cells, collected after 48h of transfection. M.O.I 1 *p 0.05 (Student's t-test).

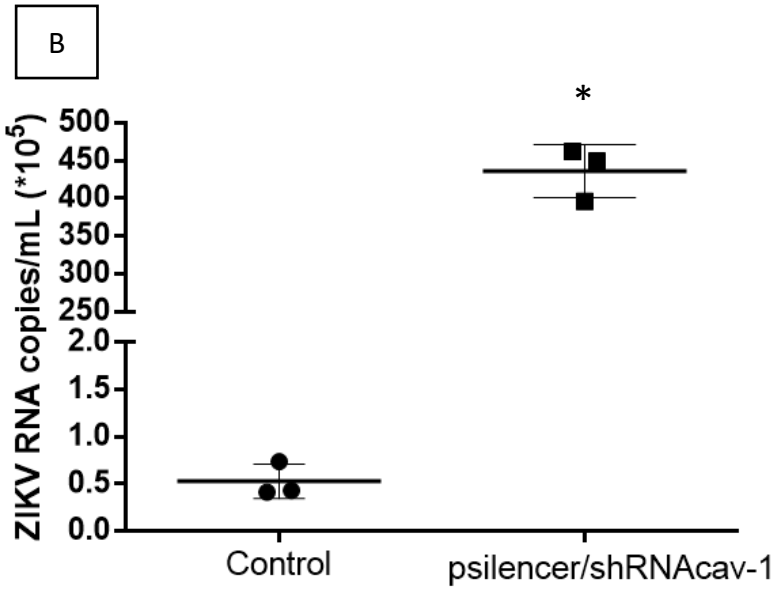

Figure 12. (B) Absolute quantification of ZIKV number of mRNA copies in control cells compared with shRNAcav-1 transfected cells, both infected after 48h of transfection, at MOI: 1 and collected after 24h post infection. *p 0.05 (Student's t-test).

With the hypothesis, still standing, that decreasing the levels of cav-1 have a positive effect for ZIKV replication (due to the results obtained in Fig.12), it was thought that, possibly, the contrary effect would be detrimental for the virus multiplication.

Therefore, it was proceeded to the evaluation of the effect of high levels of cav-1 expression upon ZIKV.

4.7 Study of cav-1 over expression using pcDNA$_3$/cav-1 construct in the context of ZIKV infection.

It was first tested if the pcDNA$_3$/cav-1 vector induced a substantial overexpression on THP-1 cells after transfection, then the infection of ZIKV with a MOI: 1 was evaluated in transfected cells expressing high levels of cav-1 mRNA. As observed in Fig.13 (A and B) the overexpression was achieved, but no difference was found in ZIKV RNA copy number inside the cell.

When the levels of cav-1 are evaluated in the context of ZIKV infection with a MOI: 5, it can be observed that on this set of experiment ZIKV did not acted as a negative modulator of cav-1 with no differences between control and infected cells, like shown in Fig 10 and 11. On the other hand, there was no significant difference on cav-1 expression on transfected cells with pcDNA$_3$/cav-1 when comparing infection vs no infection as observed in Fig. 14 (A). As when the number of ZIKV RNA

copies were quantified, the results showed, once again, a lack of detection in many of the replicates as seen in Fig. 14 (B). Finally, the plaque assay for ZIKV titration showed no differences between control and cells with overexpression for any of the studied post-infection times.

It was also decided for this system to repeat the assay with only one incubation time of 24 hours, comparing viral load of M.O.I.1 and M.O.I.5, increasing the amount of replicates to 9 per condition for ZIKV RNA quantification. The results are shown in Fig. 14.

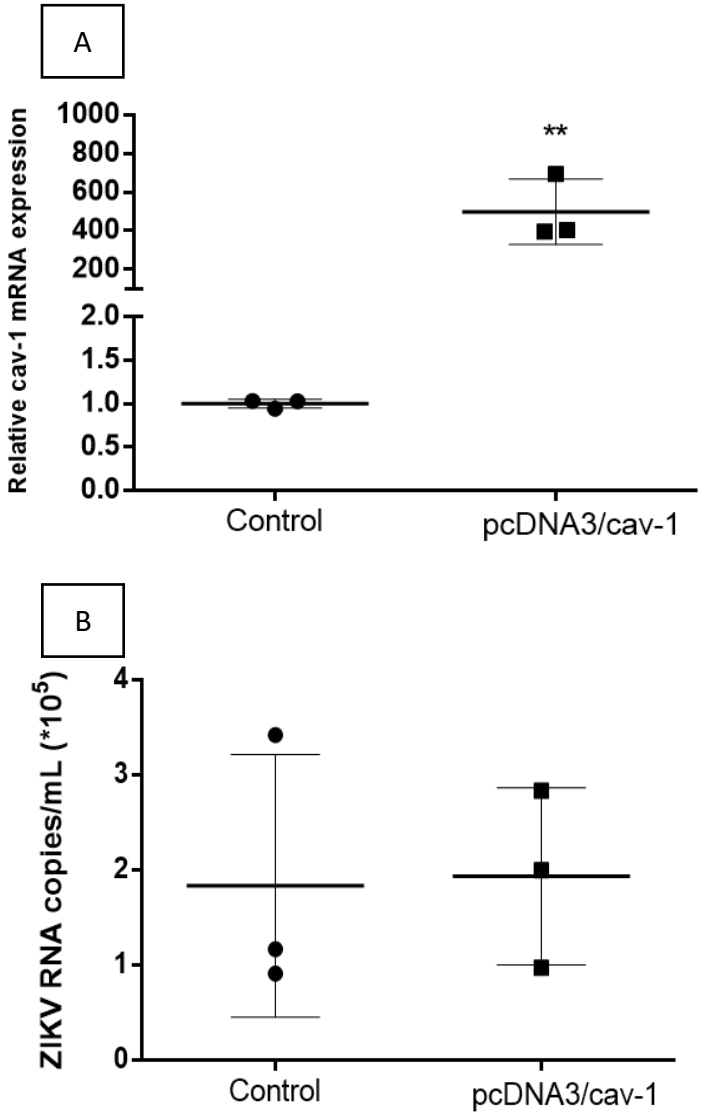

Figure 13. Study of pcDNA3/cav-1 over expression effect on infection with ZIKV using THP-1 transfected cells. Control cells were transfected with an empty plasmid (without the cav-1 mRNA sequence for over expression). **(A)** Relative quantification of expression levels of cav-1 mRNA of control cells compared with $pcDNA_3$/cav-1 transfected cells, collected after 48h of transfection. *p 0.05 (Student's t-test).
(B) Absolute quantification of ZIKV number of mRNA copies in control cells compared with $pcDNA_3$/cav-1 transfected cells, both infected after 48h of transfection, at MOI: 1 and collected after 24h post infection. *p 0.05 (Student's t-test).

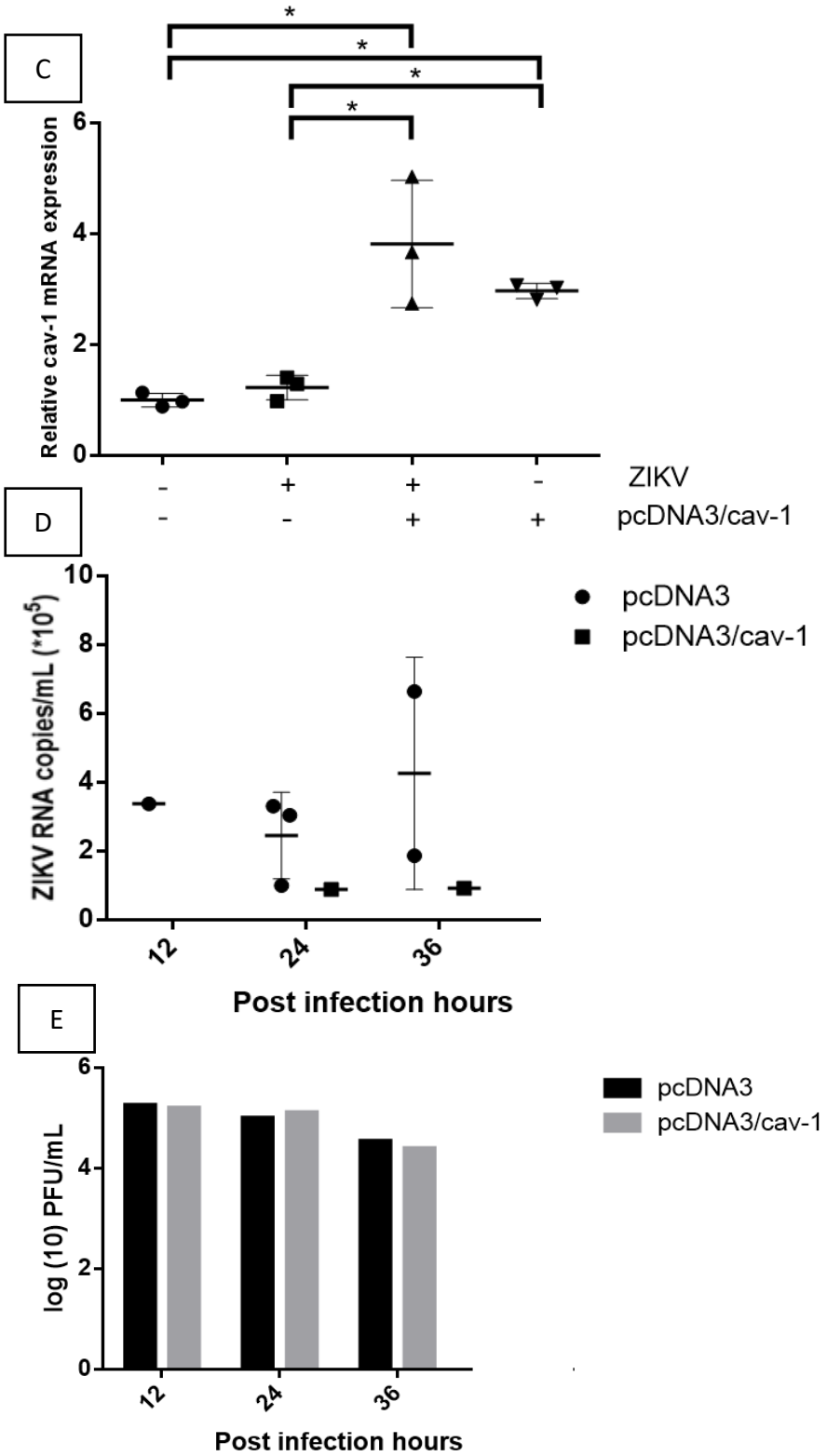

Figure 14. (A) Comparison of cav-1 mRNA expression levels between cells transfected for 48h with pcDNA3 (designated as "–" for the presence of the insert) or $pcDNA_3$/cav-1 (designated as "+" for the presence of the insert), infected or not at MOI: 5, collected after 24h of post-infection time. *p 0.05 (one-way ANOVA). **(B)** Absolute quantification of ZIKV number of mRNA copies in $pcDNA_3$ (control) transfected cells compared with $pcDNA_3$/cav-1 transfected cells, infected at MOI: 5 and collected after 12, 24 and 36h of post infection time. **(C)** ZIKV titration using plaque assay. Culture media of cells infected at a MOI: 5 were collected after 12, 24 and 36h of post infection time to determine the Plaque Forming Units (PFU) per mL.

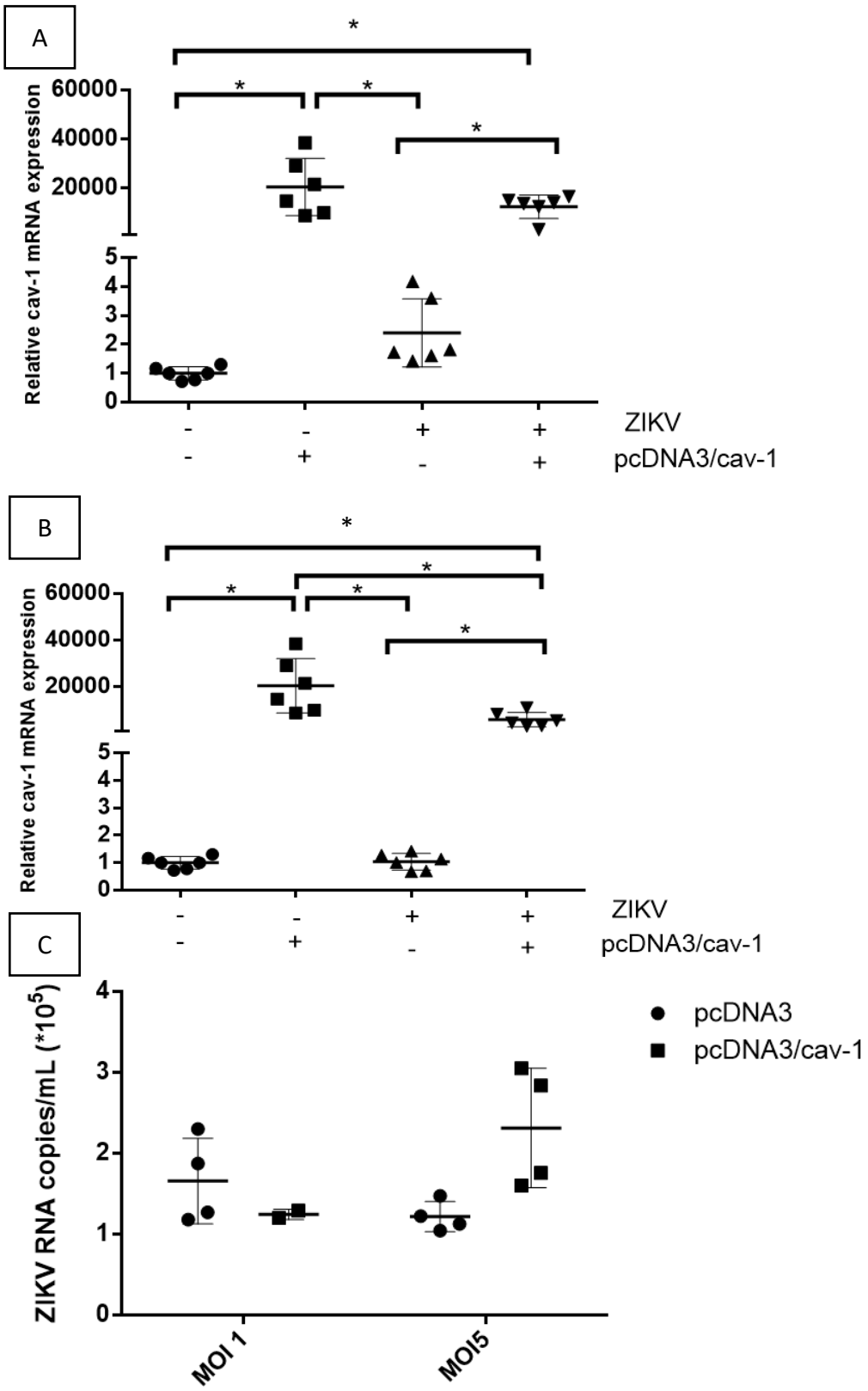

Figure 15. Study of pcDNA3/cav-1 effect on 24 hours infection with ZIKV using THP-1 transfected cells. Control cells were transfected with an empty plasmid (without the cav-1 sequence). **(A)** Comparison of cav-1 mRNA expression levels between cells transfected for 48h with $pcDNA_3$ (designated as "–" for the presence of the insert) or p $pcDNA_3$/cav-1 (designated as "+" for the presence of the insert), infected or not at MOI: 1, collected after 24h of post Infection time. *p 0.05 (one-way ANOVA). **(B)** Same conditions than A, with the difference of an increase viral load, at MOI: 5. *p 0.05 (Mann-Whitney). **(C)** Absolute quantification of ZIKV number of mRNA copies in $pcDNA_3$ (control) transfected cells compared with $pcDNA_3$/cav-1 transfected cells, infected at MOI: 1 and MOI: 5 and collected after 24h of post infection time. No difference found (2-way ANOVA).

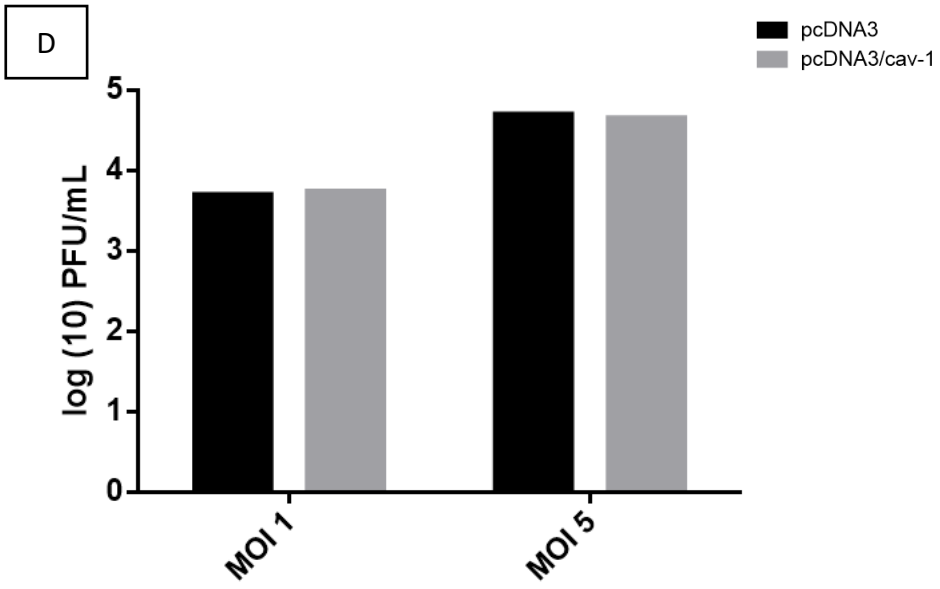

Figure 14. (E) ZIKV titration using plaque assay. Culture media of cells infected at a were collected MOI: 1 and MOI: 5 after 24h of post infection time to determine the Plaque Forming Units (PFU) per mL.

Analyzing Fig. 15 (A and B) it was found the same results as before (Fig.14 A) where transfection for a cav-1 overexpression was successfully achieved and ZIKV does not act as modulator of cav-1 expression.

For viral quantification, it was found that an increase expression of cav-1 did not influenced ZIKV replication cycle, neither for M.O.I.1 nor for M.O.I.5, as can finally be observed in Fig.15 (C). These results are supported by the titration assay of Fig.15 (D) where there is no difference stablished in the PFU of control when compared with cells with overexpression.

The limitations of overexpressing mRNA sequences by plasmid transfection is that overexpression of mRNA of one protein does not necessarily mean over expression of the protein itself, since the cell have a lot of ways to regulate the level of each protein that produces, by processes that are highly optimized to maximize cellular functionality. Therefore, if the abnormal expression of a protein can have a detrimental effect on cellular functions, the cell will activate regulation mechanisms to maintain balance (WAGNER, 2005)

Activities of regulatory molecules such as transcription factors and signaling elements are usually modulated in response to changes in external and internal cellular conditions (MORIYA, 2015) .

Cellular functions are performed through cooperative actions of thousands of proteins. Intracellular levels of these proteins vary substantially trough processes like resource overload, stoichiometric imbalance, promiscuous interactions, and pathway modulation (TOMALA; KORONA, 2013). Due to a mass-action effect, overexpression might cause activation/inactivation of their target pathways leading the cell to a normal production of the target protein when there is still high levels of its mRNA inside the cell. Such pathway modulations have been repeatedly observed in individual overexpression experiments (PRELICH, 2012).

In order to confirm that the overexpression of cav-1 mRNA is being traduced in its majority to protein, it is necessary to perform several more experiments, like Western Blot or fluorescent microscopy to be able of properly show that indeed high levels of cav-1 do not affect ZIKV replication. Until now, it is still not clear, even when these primarily results are pointing in that direction.

5 Conclusions.

Cells with cholesterol depletion from cell membranes lowers the production of ZIKV, suggesting that cholesterol content in cell membrane is important in the ZIKV replication cycle. ZIKV may be a negative modulator for cav-1 protein expression in THP-1 cells upon infection. Neither cav-1 silencing nor overexpression showed any consistent effect on ZIKV replication.

6 Perspectives.

- Standardize the transfection procedure in order to obtain a complete knockdown of cav-1 inside the cells, to achieve reproducible results and continue to study its possible effect on ZIKV replication.
- Perform Western Blot or fluorescent microscopy to properly show that indeed high levels of cav-1 do not affect ZIKV replication.
- Generate of stable clones of adherent human cells with psingle/shRNAm and pSilencer/shRNAm vectors to obtain higher quantity and quality of mRNA that should produce results with less variation between samples.

7 Cited Literature.

ABECASIS, A. B.; PIMENTEL, V.; PINGARILHO, M. An updated genotype classification system for Zika viruses. **bioRxiv**, v. 760066, 2019.

AKTEPE, T. E.; MACKENZIE, J. M. Shaping the flavivirus replication complex: It is curvaceous! **Cellular Microbiology**, v. 20, n. 8, p. 1–10, 2018.

ALVARADO, M. G.; SCHWARTZ, D. A. Zika virus infection in pregnancy, microcephaly, and maternal and fetal health: What we think, what we know, and what we think we know. **Archives of Pathology and Laboratory Medicine**, v. 141, n. 1, p. 26–32, 2017.

AMERES, S. L.; MARTINEZ, J.; SCHROEDER, R. Molecular Basis for Target RNA Recognition and Cleavage by Human RISC. **Cell**, v. 130, n. 1, p. 101–112, 2007.

BARMAN, S.; NAYAK, D. P. Lipid Raft Disruption by Cholesterol Depletion Enhances Influenza A Virus Budding from MDCK Cells. **Journal of Virology**, v. 81, n. 22, p. 12169–12178, 2007.

BAYLESS, N. L. et al. Zika Virus Infection Induces Cranial Neural Crest Cells to Produce Cytokines at Levels Detrimental for Neurogenesis. **Cell Host and Microbe**, v. 20, n. 4, p. 423–428, 2016.

BERNS, K. et al. A large-scale RNAi screen in human cells identifies new components of the p53 pathway. **Nature**, v. 428, n. 6981, p. 431–437, 2004.

BIPHENYLS, C. P. Potential for Treatment and a Zika Virus Vaccine Natalie. v. 91, n. 2, p. 165–171, 2015.

CAMARGOS, V. N. et al. In-depth characterization of congenital Zika syndrome in immunocompetent mice: Antibody-dependent enhancement and an antiviral peptide therapy. **EBioMedicine**, v. 44, p. 516–529, 2019.

CHAMBERS, T. J. et al. AND REPLICATION ORGJ \ NIZATION , EXPRESSION , l. **Genome**, 1990.

CHAN, J. F. W. et al. Differential cell line susceptibility to the emerging Zika virus: implications for disease pathogenesis, non-vector-borne human transmission and animal reservoirs. **Emerging microbes & infections**, v. 5, n. August, p. e93, 2016.

CHO, J. S.; KIM, Y. C.; MORRISON, S. L. Inhibitors of MyD88-dependent proinflammatory cytokine production identified utilizing a novel RNA interference screening approach. **PLoS ONE**, v. 4, n. 9, 2009.

CHRIS B. MOORE, ELIZABETH H. GUTHRIE, MAX TZE-HAN HUANG, AND D. J. T. RNA therapeutics: function, design, and delivery. Preface. **Methods in molecular biology (Clifton, N.J.)**, v. 629, n. 2, p. 141–158, 2010.

CORDERO, J. G. et al. Caveolin-1 in lipid rafts interacts with dengue virus NS3 during polyprotein processing and replication in HMEC-1 cells. **PLoS ONE**, v. 9, n. 3, p. 1–10, 2014.

DAS, S.; CHAKRABORTY, S.; BASU, A. Critical role of lipid rafts in virus entry and activation of phosphoinositide 3’ kinase/Akt signaling during early stages of Japanese encephalitis virus infection in neural stem/progenitor cells. **Journal of Neurochemistry**, v. 115, n. 2, p. 537–549, 2010.

DIAZ-VALDIVIA, N. et al. Enhanced caveolin-1 expression increases migration, anchorage-independent growth and invasion of endometrial adenocarcinoma cells. **BMC Cancer**, v. 15, n. 1, p. 1–11, 2015.

DIDIER MUSSO AND DUANE J. GUBLER. Zika Virus. **Nature**, v. 11, n. 1, p. 10–20, 2016.

DOU, X. et al. Cholesterol of lipid rafts is a key determinant for entry and post-entry control of porcine rotavirus infection. **BMC Veterinary Research**, v. 14, n. 1, p. 1–12, 2018.

DREJA, K. et al. Cholesterol depletion disrupts caveolae and differentially impairs agonist-induced arterial contraction. **Arteriosclerosis, Thrombosis, and Vascular Biology**, v. 22, n. 8, p. 1267–1272, 2002.

ESPAÑO, E. et al. Lipophilic statins inhibit Zika virus production in Vero cells. **Scientific Reports**, v. 9, n. 11461, p. 1–11, 2019.

FAN CHENG,A SUZANE RAMOS DA SILVA,A I-CHUEH HUANG,A JAE U. JUNG,A SHOU-JIANG GAOA, B A. Suppression of Zika Virus Infection and Replication in. **Jounal of Virology**, v. 92, n. 4, p. 1–17, 2018.

FELLMANN, C. et al. Functional Identification of Optimized RNAi Triggers Using a Massively Parallel Sensor Assay. **Molecular Cell**, v. 41, n. 6, p. 733–746, 2011.

FIUCCI, G. et al. Caveolin-1 inhibits anchorage-independent growth, anoikis and invasiveness in MCF-7 human breast cancer cells. **Oncogene**, v. 21, n. 15, p. 2365–2375, 2002.

GARCIA-BLANCO, M. A. et al. Flavivirus RNA transactions from viral entry to genome replication. **Antiviral Research**, v. 134, p. 244–249, 2016.

GAUS, K. et al. Domain-specific lipid distribution in macrophage plasma membranes. **Journal of Lipid Research**, v. 46, n. 7, p. 1526–1538, 2005.

GOMEZ-MARTINEZ, M.; SCHMITZ, D.; HERGOVICH, A. Generation of stable human cell lines with tetracycline-inducible (Tet-on) shRNA or cDNA expression. **Journal of Visualized Experiments**, n. 73, p. 1–7, 2013.

GONZALEZ, E. et al. Small interfering RNA-mediated down-regulation of caveolin-1 differentially modulates signaling pathways in endothelial cells. **Journal of Biological Chemistry**, v. 279, n. 39, p. 40659–40669, 2004.

GUTIÉRREZ-BUGALLO, G. et al. Vector-borne transmission and evolution of Zika virus. **Nature Ecology and Evolution**, v. 3, n. 4, p. 561–569, 2019.

HEALE, B. S. E. et al. siRNA target site secondary structure predictions using local stable substructures. **Nucleic Acids Research**, v. 33, n. 3, p. 1–10, 2005.

HENNESSEY, M.; FISCHER, M.; STAPLES, J. Zika Virus Spreads to New Areas — Region of the Americas. **MMWR Morbidity and Mortality Weekly Report**, v. 65, n. May 2015, p. 55–8, 2016.

HOHENWARTER, L. **Distribution of RNAs via the exosomal pathway**, 2017.

HYOCHOL AHN, PHD, MICHAEL WEAVER, PHD, DEBRA LYON, PHD, EUNYOUNG CHOI, RN, AND ROGER B. FILLINGIM, P. p38MAPK plays a critical role in induction of a pro-inflammatory phenotype of retinal Müller cells following Zika virus infection. **Physiology & behavior**, v. 176, n. 10, p. 139–148, 2017.

JAIN, H. et al. Knockdown of the myostatin gene by RNA interference in caprine fibroblast cells. **Journal of Biotechnology**, v. 145, n. 2, p. 99–102, 2010.

KHVOROVA, A.; REYNOLDS, A.; JAYASENA, S. D. Functional siRNAs and miRNAs exhibit strand bias. **Cell**, v. 115, n. 2, p. 209–216, 2003.

KILSDONK, E. P. C. et al. **Cellular cholesterol efflux mediated by cyclodextrinsJournal of Biological Chemistry**, 1995.

LEE, C.-J. et al. Cholesterol Effectively Blocks Entry of Flavivirus. **Journal of Virology**, v. 82, n.

13, p. 6470–6480, 2008a.

LEE, I. et al. Probing molecular insights into Zika virus–host interactions. **Viruses**, v. 10, n. 5, p. 1–26, 2018.

LEE, Y. et al. Signaling Pathways Involved In Dengue-2 Virus Infection Induced RANTES Overexpression Institute of Basic Medical Sciences Medical Laboratory Science and Biotechnologyand Pediatrics College of Medicine , National Cheng Kung University. **American Journal of Infectious Diseases**, v. 4, n. 1, p. 32–40, 2008b.

LEVITAN, I. et al. Membrane cholesterol content modulates activation of volume-regulated anion current in bovine endothelial cells. **Journal of General Physiology**, v. 115, n. 4, p. 405–416, 2000.

MACKENZIE, J. M.; KHROMYKH, A. A.; PARTON, R. G. Cholesterol Manipulation by West Nile Virus Perturbs the Cellular Immune Response. **Cell Host and Microbe**, v. 2, n. 4, p. 229–239, 2007.

MAHAMMAD, S.; PARMRYD, I. Cholesterol depletion using methyl-β-cyclodextrin. **Methods in molecular biology (Clifton, N.J.)**, v. 1232, p. 91–102, 2015.

MARTÍN-ACEBES, M. A. et al. West nile virus replication requires fatty acid synthesis but is independent on phosphatidylinositol-4-phosphate lipids. **PLoS ONE**, v. 6, n. 9, 2011.

MARTÍN-ACEBES, M. A.; VÁZQUEZ-CALVO, Á.; SAIZ, J. C. Lipids and flaviviruses, present and future perspectives for the control of dengue, Zika, and West Nile viruses. **Progress in Lipid Research**, v. 64, p. 123–137, 2016.

MEDIGESHI, G. R. et al. West Nile Virus Entry Requires Cholesterol-Rich Membrane Microdomains and Is Independent of v 3 Integrin. **Journal of Virology**, v. 82, n. 11, p. 5212–5219, 2008.

MORIYA, H. Quantitative nature of overexpression experiments. **Molecular Biology of the Cell**, v. 26, n. 22, p. 3932–3939, 2015.

OSUNA-RAMOS, J. F.; REYES-RUIZ, J. M.; DEL ÁNGEL, R. M. The Role of Host Cholesterol During Flavivirus Infection. **Frontiers in cellular and infection microbiology**, v. 8, n. November, p. 388, 2018.

PEÑA, J.; HARRIS, E. Early dengue virus protein synthesis induces extensive rearrangement of the endoplasmic reticulum independent of the UPR and SREBP-2 pathway. **PLoS ONE**, v. 7, n. 6, p. 1–15, 2012.

PRALLE, A. et al. Sphingolipid-cholesterol rafts diffuse as small entities in the plasma membrane of mammalian cells. **Journal of Cell Biology**, v. 148, n. 5, p. 997–1007, 2000.

PREDESCU, S. A. et al. Cholesterol-dependent syntaxin-4 and SNAP-23 clustering regulates caveolar fusion with the endothelial plasma membrane. **Journal of Biological Chemistry**, v. 280, n. 44, p. 37130–37138, 2005.

PRELICH, G. Gene overexpression: Uses, mechanisms, and interpretation. **Genetics**, v. 190, n. 3, p. 841–854, 2012.

REYNOLDS, A. et al. Rational siRNA design for RNA interference. **Nature Biotechnology**, v. 22, n. 3, p. 326–330, 2004.

ROOSENDAAL, J. et al. Regulated Cleavages at the West Nile Virus NS4A-2K-NS4B Junctions Play a Major Role in Rearranging Cytoplasmic Membranes and Golgi Trafficking of the NS4A Protein. **Journal of Virology**, v. 80, n. 9, p. 4623–4632, 2006.

RYAN, S. J. et al. Global expansion and redistribution of Aedes-borne virus transmission risk with climate change. **PLoS Neglected Tropical Diseases**, v. 13, n. 3, p. 1–20, 2018.

SAGER, G. et al. Role of host cell secretory machinery in zika virus life cycle. **Viruses**, v. 10, n. 10, p. 2013–2014, 2018.

SANDY, P.; VENTURA, A.; JACKS, T. Mammalian RNAi: A practical guide. **BioTechniques**, v. 39, n. 2, p. 215–224, 2005.

SCATURRO, P. et al. An orthogonal proteomic survey uncovers novel Zika virus host factors. **Nature**, v. 561, n. 7722, p. 253–257, 2018.

SCHERER, L. J. et al. Rapid assessment of anti-HIV siRNA efficacy using PCR-derived Pol III shRNA cassettes. **Molecular Therapy**, v. 10, n. 3, p. 597–603, 2004.

SCHWARZ, D. S. et al. Asymmetry in the assembly of the RNAi enzyme complex. **Cell**, v. 115, n. 2, p. 199–208, 2003.

SHAH, M. et al. Interactions of STAT3 with caveolin-1 and heat shock protein 90 in plasma membrane raft and cytosolic complexes: Preservation of cytokine signaling during fever. **Journal of Biological Chemistry**, v. 277, n. 47, p. 45662–45669, 2002.

SHEETS, E. D.; HOLOWKA, D.; BAIRD, B. Critical Role for Cholesterol in Lyn-mediated Tyrosine Phosphorylation of FceRI and Their Association with Detergent-resistant Membranes. **The Journal of Cell Biology**, v. 145, n. 4, p. 877–887, 1999.

SHI, S. T. et al. Hepatitis C Virus RNA Replication Occurs on a Detergent-Resistant Membrane That Cofractionates with Caveolin-2. **Journal of Virology**, v. 77, n. 7, p. 4160–4168, 2003.

SIMONS, K.; SAMPAIO, J. L. Membrane organization and lipid rafts. **Cold Spring Harbor Perspectives in Biology**, v. 3, n. 10, p. 1–17, 2011.

STAPLEFORD, K. A.; MILLER, D. J. Role of cellular lipids in positive-sense RNA virus replication complex assembly and function. **Viruses**, v. 2, n. 5, p. 1055–1068, 2010.

STIASNY, K.; KOESSL, C.; HEINZ, F. X. Involvement of Lipids in Different Steps of the Flavivirus Fusion Mechanism. **Journal of Virology**, v. 77, n. 14, p. 7856–7862, 2003.

SUN, X.; WHITTAKER, G. R. Role for Influenza Virus Envelope Cholesterol in Virus Entry and Infection. **Journal of Virology**, v. 77, n. 23, p. 12543–12551, 2003.

TANI, H. et al. Involvement of Ceramide in the Propagation of Japanese Encephalitis Virus. **Journal of Virology**, v. 84, n. 6, p. 2798–2807, 2010.

TOMALA, K.; KORONA, R. Evaluating the fitness cost of protein expression in saccharomyces cerevisiae. **Genome Biology and Evolution**, v. 5, n. 11, p. 2051–2060, 2013.

UPLA, P.; HYYPIÄ, T.; MARJOMÄKI, V. Role of lipid rafts in virus infection. **Future Virology**, v. 4, n. 5, p. 487–500, 2009.

VENTURI, G. et al. Epidemiological and clinical suspicion of congenital Zika virus infection: Serological findings in mothers and children from Brazil. **Journal of Medical Virology**, v. 91, n. 9, p. 1577–1583, 2019.

VERT, J. P. et al. An accurate and interpretable model for siRNA efficacy prediction. **BMC Bioinformatics**, v. 7, p. 1–17, 2006.

VICTORIA PORTNOY, VERA HUANG, ROBERT F. PLACE, AND L.-C. L. Small RNA and transcriptional upregulation. **wiley Interdiscip Rev RNA**, v. 2, n. 5, p. 748–760, 2011.

WAGNER, A. Energy constraints on the evolution of gene expression. **Molecular Biology and**

Evolution, v. 22, n. 6, p. 1365–1374, 2005.

WANG, X. JUN et al. A Simple and Robust Vector-Based shRNA Expression System Used for RNA Interference. **PLoS ONE**, v. 8, n. 2, 2013.

WELSCH, S. et al. Composition and Three-Dimensional Architecture of the Dengue Virus Replication and Assembly Sites. **Cell Host and Microbe**, v. 5, n. 4, p. 365–375, 2009.

WENG, Y. et al. A multi-shRNA vector enhances the silencing efficiency of exogenous and endogenous genes in human cells. **Oncology Letters**, v. 13, n. 3, p. 1553–1562, 2017.

XING, H. et al. Activation of fibronectin/PI-3K/Akt2 leads to chemoresistance to docetaxel by regulating survivin protein expression in ovarian and breast cancer cells. **Cancer Letters**, v. 261, n. 1, p. 108–119, 2008.

YIN, H. et al. Caveolin proteins: a molecular insight into disease. **Frontiers of Medicine**, v. 10, n. 4, p. 397–404, 2016.

ZANLUCA, C.; DOS SANTOS, C. N. D. Zika virus – an overview. **Microbes and Infection**, v. 18, n. 5, p. 295–301, 2016.

ZHONG, Y. BIN et al. First case of laboratory-confirmed zika virus infection imported into China. **Chinese Medical Journal**, v. 129, n. 16, p. 2013–2014, 2016.

ZIDOVETZKI, R.; LEVITAN, I. Use of cyclodextrins to manipulate plasma membrane cholesterol content: evidence, misconceptions and control strategies. **Biochimica et Biophysica Acta (BBA) - Biomembranes**, v. 1768, n. 6, p. 1311–1324, 2007.

8 Attachments

8.1 Vector for psingle

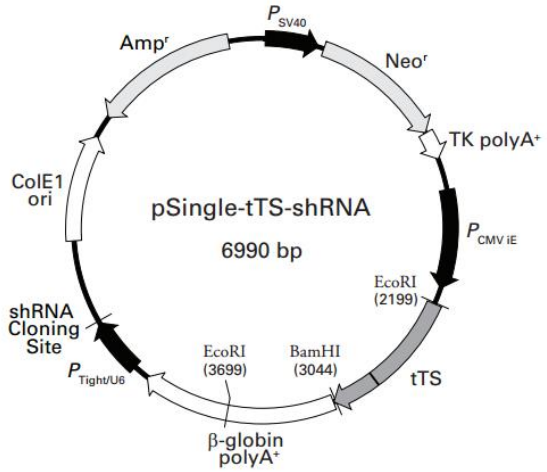


```
4641                XhoI        HindIII                    XhoI        HindIII                4730
5'-GAAAGGACGA CTCGAGGGAC AAGCTTATCT - 30 bp - ACTCGAGGGA CAAGCTTATC TATGTCGGGT-3'
3'-CTTTCCTGCT GAGCTCCCTG TTCGAATAGA --------- TGAGCTCCCT GTTCGAATAG ATACAGCCCA-5'
```

pSingle-tTS-shRNA vector map and shRNA cloning site. Complete digestion of the vector with XhoI and HindIII results in the removal of the nucleotides indicated in gray in the above shRNA cloning site. The XhoI/HindIII digested vector will accept annealed ds shRNA oligonucleotides with the corresponding XhoI and HindIII overhangs.

8.2 Vector for pSilencer

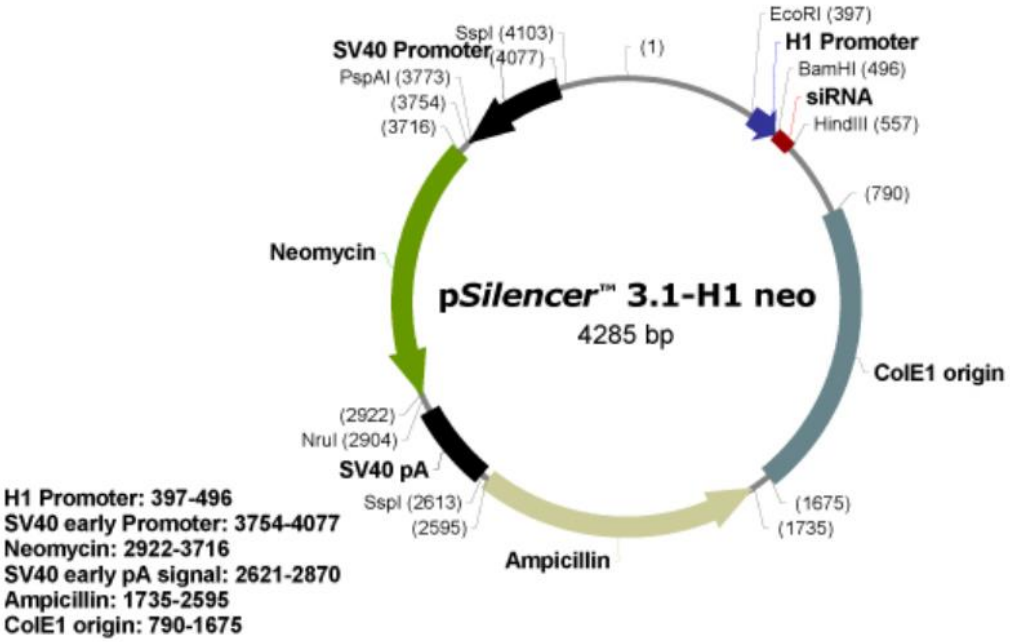

8.3 Vector for pcDNA$_3$

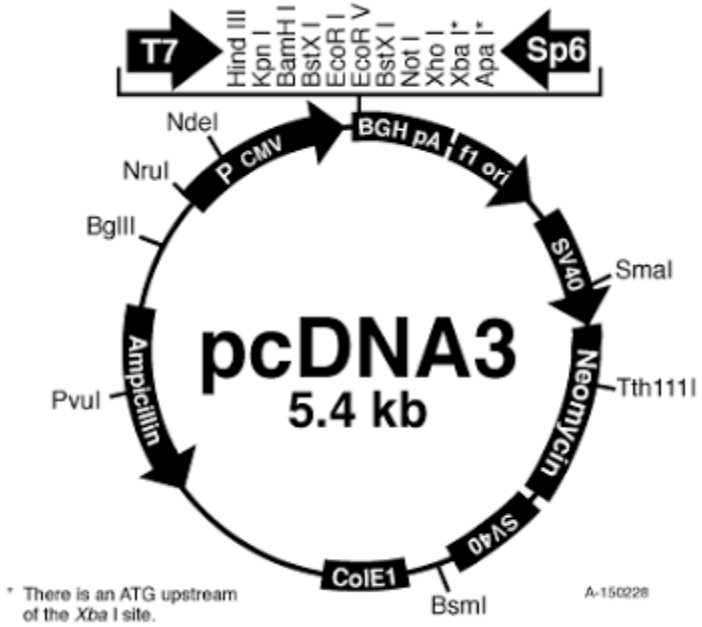

9 Appendix

9.1 Transformation system for cav-1 silencing: psingle vector digestion

1) Molecular Weight marker 1kb

2) Digested plasmid

3) Undigested plasmid

9.2 Transformation system for cav-1 over expression: Insert (gBlock) digestion

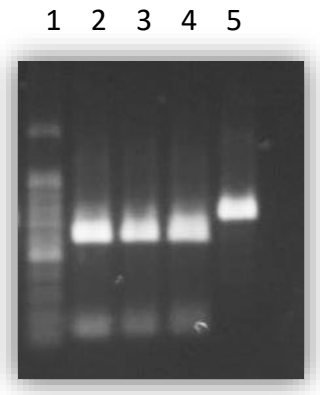

1) Molecular Weight marker 0.1kb

2-4) Digested gblock cav-1

5) Undigested gblock cav-1

1) Molecular Weight marker 0.1kb

2-4) Digested plasmid

5) Undigested plasmid

9.3 Transformed colonies

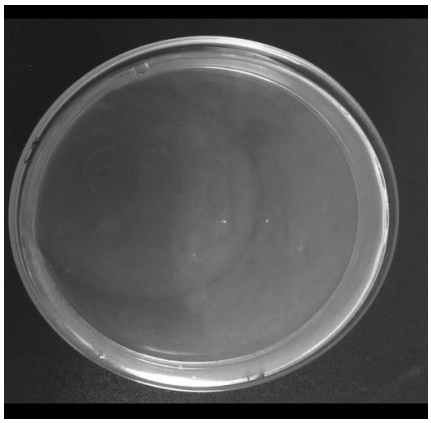

Control

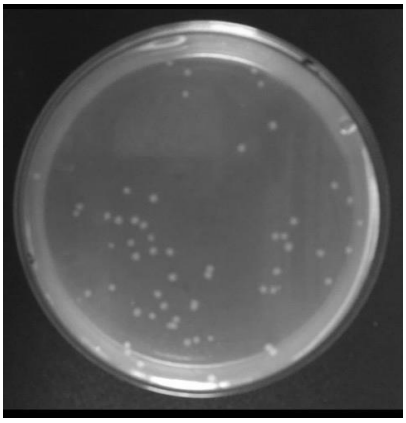

Transformed colonies

9.4 Colony PCR

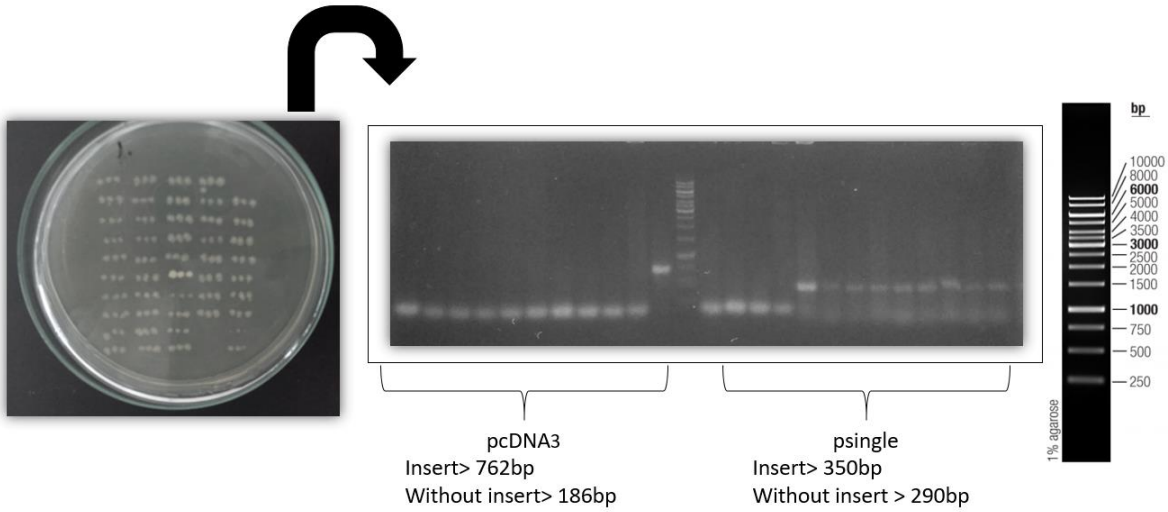

9.5 Electrophoresis for plasmid recovery confirmation

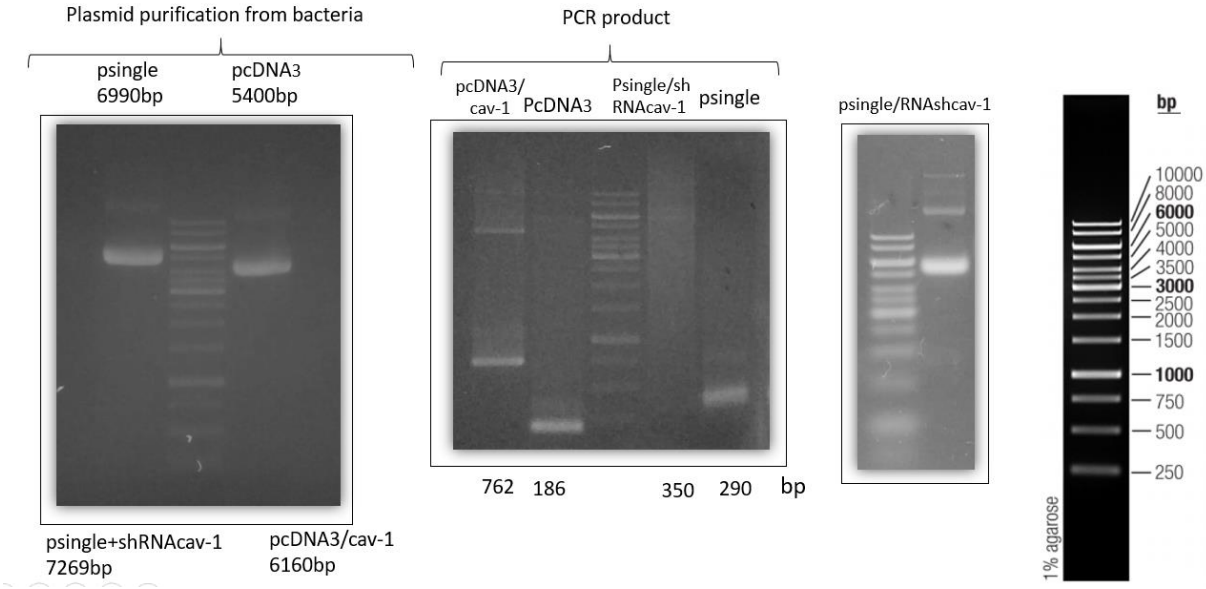

9.6 Statistical analysis

9.6.1 Kruskall Wallis analysis of Figure 6.A (Viable number of cells after several concentrations of MβCD treatment) with multiple comparisons using 1 one-way ANOVA.

```
Number of families      1
Number of comparisons per family        10
Alpha   0,05

Dunn's multiple comparisons test        Mean rank diff, Significant?    Summary

  Control  vs. 5        -6,000  No      ns
  Control  vs. 10       -3,000  No      ns
  Control  vs. 15       -10,33  Yes     *
  Control  vs. 20       -10,67  Yes     *
  5 vs. 10      3,000   No      ns
  5 vs. 15      -4,333  No      ns
  5 vs. 20      -4,667  No      ns
  10 vs. 15     -7,333  No      ns
  10 vs. 20     -7,667  No      ns
  15 vs. 20     -0,3333 No      ns


Test details    Mean rank 1     Mean rank 2     Mean rank diff, n1      n2

  Control  vs. 5        2,000   8,000   -6,000  3       3
  Control  vs. 10       2,000   5,000   -3,000  3       3
  Control  vs. 15       2,000   12,33   -10,33  3       3
  Control  vs. 20       2,000   12,67   -10,67  3       3
  5 vs. 10      8,000   5,000   3,000   3       3
  5 vs. 15      8,000   12,33   -4,333  3       3
  5 vs. 20      8,000   12,67   -4,667  3       3
  10 vs. 15     5,000   12,33   -7,333  3       3
  10 vs. 20     5,000   12,67   -7,667  3       3
  15 vs. 20     12,33   12,67   -0,3333 3       3
```

9.6.2 2way ANOVA analysis of Figure 6.B (Effects of MβCD treatment on cellular cholesterol level)

```
Compare row means (main row effect)

Number of families      1
Number of comparisons per family        4
Alpha   0,05

Sidak's multiple comparisons test       Mean Diff,      95% CI of diff, Significant?    Summary

  Control  vs. 5        0,05167 -0,1124 to 0,2158       No      ns
  Control  vs. 10       0,1067  -0,05743 to 0,2708      No      ns
  Control  vs. 15       0,3083  0,1442 to 0,4724        Yes     ***
  Control  vs. 20       0,7917  0,6276 to 0,9558        Yes     ****


Test details    Mean 1  Mean 2  Mean Diff,      SE of diff,     N1      N2      t       DF

  Control  vs. 5        2,042   1,990   0,05167 0,05421 6       6       0,9531  10
  Control  vs. 10       2,042   1,935   0,1067  0,05421 6       6       1,968   10
  Control  vs. 15       2,042   1,733   0,3083  0,05421 6       6       5,688   10
  Control  vs. 20       2,042   1,250   0,7917  0,05421 6       6       14,60   10
```

9.6.3 T test Analysis of Figure 7. A (Comparison of expression levels of RNAm cav-1 on MβCD treated cells, infected or not with ZIKV).

```
Column B        ZIKV+
vs.     vs,
Column A        ZIKV-

Unpaired t test
  P value       0,1097
  P value summary       ns
  Significantly different? (P < 0.05)   No
  One- or two-tailed P value?   One-tailed
  t, df t=1,455 df=4

How big is the difference?
  Mean ± SEM of column A        0,2086 ± 0,02544 N=3
  Mean ± SEM of column B        0,2730 ± 0,03622 N=3
  Difference between means      0,06439 ± 0,04426
  95% confidence interval       -0,05850 to 0,1873
  R square      0,3460

F test to compare variances
  F,DFn, Dfd    2,027, 2, 2
  P value       0,6607
  P value summary       ns
  Significantly different? (P < 0.05)   No

Model comparison        SS      DF      Probability it is correct
  Null H. Population means identical    0,01797 5       97,65%
  Alternative H: Distinct population means      0,01175 4       2,35%
  Ratio of probabilities                        41,51
  Difference in AICc                    -7,452
```

9.6.4 T test Analysis of Figure 716.B (Comparison of ZIKV RNA levels between not treated and treated cells). ZIKV RNA copies was significantly reduced upon MβCD treatment.

```
Column B        BMCD+
vs.     vs,
Column A        BMCD-

Unpaired t test
  P value       0,0051
  P value summary       **
  Significantly different? (P < 0.05)   Yes
  One- or two-tailed P value?   One-tailed
  t, df t=4,576 df=4

How big is the difference?
  Mean ± SEM of column A        1,306 ± 0,09420 N=3
  Mean ± SEM of column B        0,3812 ± 0,1788 N=3
  Difference between means      -0,9247 ± 0,2021
  95% confidence interval       -1,486 to -0,3636
  R square      0,8396

F test to compare variances
  F,DFn, Dfd    3,602, 2, 2
  P value       0,4346
  P value summary       ns
  Significantly different? (P < 0.05)   No

Model comparison        SS      DF      Probability it is correct
  Null H. Population means identical    1,528   5       37,98%
  Alternative H: Distinct population means      0,2450  4       62,02%
  Ratio of probabilities                        1,633
  Difference in AICc                    0,9810
```

9.6.5 T test analysis of Figure 8 (Comparison of levels of expression of cav-1 mRNA on THP-1 infected or not with ZIKV)

```
Table Analyzed  Infection vs no infection

Column B        Control
vs.     vs,
Column A        ZIKV+

Unpaired t test
  P value       0,0008
  P value summary       ***
  Significantly different? (P < 0.05)   Yes
  One- or two-tailed P value?   One-tailed
  t, df t=7,490 df=4

How big is the difference?
  Mean ± SEM of column A        0,2941 ± 0,01745 N=3
  Mean ± SEM of column B        1,133 ± 0,1107 N=3
  Difference between means      0,8393 ± 0,1121
  95% confidence interval       0,5281 to 1,150
  R square      0,9334

F test to compare variances
  F,DFn, Dfd    40,21, 2, 2
  P value       0,0485
  P value summary       *
  Significantly different? (P < 0.05)   Yes

Model comparison        SS      DF      Probability it is correct
  Null H. Population means identical    1,132   5       4,19%
  Alternative H: Distinct population means      0,07534 4       95,81%
  Ratio of probabilities                        22,85
  Difference in AICc                    6,258
```

9.6.6 T test analysis of Figure 9. A (Evaluation of psingle/shRNAcav-1 effect after induction of transfected THP-1 cells). 24h of incubation with 1µg/mL of Tet.

```
Column B        control
vs.     vs,
Column A        psingle/shcav-1

Unpaired t test
  P value       0,0525
  P value summary       ns
  Significantly different? (P < 0.05)   No
  One- or two-tailed P value?   One-tailed
  t, df t=2,088 df=4

How big is the difference?
  Mean ± SEM of column A        3,163 ± 1,019 N=3
  Mean ± SEM of column B        1,000 ± 0,1868 N=3
  Difference between means      -2,163 ± 1,036
  95% confidence interval       -5,039 to 0,7133
  R square      0,5215

F test to compare variances
  F,DFn, Dfd    29,74, 2, 2
  P value       0,0651
  P value summary       ns
  Significantly different? (P < 0.05)   No

Model comparison        SS      DF      Probability it is correct
  Null H. Population means identical    13,45   5       94,21%
  Alternative H: Distinct population means      6,438   4       5,79%
  Ratio of probabilities                        16,26
  Difference in AICc                    -5,578
```

9.6.7 2 way ANOVA analysis of Figure 9.B. Evaluation of psingle silencing over time.

```
Two-way ANOVA   Ordinary
Alpha   0,05

Source of Variation     % of total variation    P value P value summary Significant?
  Interaction   19,11   < 0,0001        ****    Yes
  time post induction   24,51   < 0,0001        ****    Yes
  inductor concentration        54,23   < 0,0001        ****    Yes

ANOVA table     SS      DF      MS      F (DFn, DFd)    P value
  Interaction   83947   9       9327    F (9, 31) = 35,22       P < 0,0001
  time post induction   107679  3       35893   F (3, 31) = 135,5       P < 0,0001
  inductor concentration        238228  3       79409   F (3, 31) = 299,9       P < 0,0001
  Residual      8209    31      264,8

Number of missing values        1
```

9.6.8 One-way ANOVA analysis of Figure 10.A. Evaluation of silencing effect using pSilencer/shRNAcav-1 on infected cells MOI: 5 and 24h of postinfection time

```
ANOVA summary
  F     23,65
  P value       0,0002
  P value summary       ***
  Are differences among means statistically significant? (P < 0.05)     Yes
  R square      0,8987

Brown-Forsythe test
  F (DFn, DFd)  0,5673 (3, 8)
  P value       0,6519
  P value summary       ns
  Significantly different standard deviations? (P < 0.05)       No

Bartlett's test
  Bartlett's statistic (corrected)
  P value
  P value summary
  Significantly different standard deviations? (P < 0.05)

ANOVA table     SS      DF      MS      F (DFn, DFd)    P value
  Treatment (between columns)   1,170   3       0,3901  F (3, 8) = 23,65        P = 0,0002
  Residual (within columns)     0,1320  8       0,01649
  Total 1,302   11

Data summary
  Number of treatments (columns)        4
  Number of values (total)      12

Number of families      1
Number of comparisons per family        3
Alpha   0,05

Dunnett's multiple comparisons test     Mean Diff,      95% CI of diff, Significant?    Summary

  Control  vs. psilencer/shRNAcav-1     0,3532  0,05125 to 0,6552       Yes     *
  Control  vs. ZIKV     0,8540  0,5520 to 1,156 Yes     ***
  Control  vs. psilencer/shRNAcav-1 ZIKV        0,5730  0,2710 to 0,8750        Yes     **


Test details    Mean 1  Mean 2  Mean Diff,      SE of diff,     n1      n2      q       DF

  Control  vs. psilencer/shRNAcav-1     1,201   0,8477  0,3532  0,1049  3       3       3,368   8
  Control  vs. ZIKV     1,201   0,3469  0,8540  0,1049  3       3       8,144   8
  Control  vs. psilencer/shRNAcav-1 ZIKV        1,201   0,6279  0,5730  0,1049  3       3       5,464   8
```

9.6.9 2-way ANOVA analysis of Figure 10. B. Study of pSilencer/shRNAcav-1 silencing effect on infection with ZIKV at M.O.I.5 over time.

```
Two-way ANOVA   Ordinary
Alpha   0,05

Source of Variation     % of total variation    P value P value summary Significant?
  Interaction   2,942   0,8556  ns      No
  Row Factor    24,15   0,3231  ns      No
  Column Factor 3,765   0,5413  ns      No

ANOVA table     SS      DF      MS      F (DFn, DFd)    P value
  Interaction   0,4213  2       0,2107  F (2, 8) = 0,1591       P = 0,8556
  Row Factor    3,457   2       1,729   F (2, 8) = 1,305        P = 0,3231
  Column Factor 0,5390  1       0,5390  F (1, 8) = 0,4071       P = 0,5413
  Residual      10,59   8       1,324

Compare each cell mean with the other cell mean in that row.

Number of families      1
Number of comparisons per family        3
Alpha   0,05

Sidak's multiple comparisons test       Mean Diff,      95% CI of diff, Significant?    Summary

  Control  - psilencer/shRNAcav-1
    12  0,04070 -2,782 to 2,864 No      ns
    24  -0,8848 -5,119 to 3,350 No      ns
    36  -0,4276 -3,584 to 2,729 No      ns


Test details    Mean 1  Mean 2  Mean Diff,      SE of diff,     N1      N2      t       DF

  Control  - psilencer/shRNAcav-1
    12  2,498   2,457   0,04070 0,9396  3       3       0,04331 8
    24  0,6666  1,551   -0,8848 1,409   1       2       0,6278  8
    36  1,824   2,252   -0,4276 1,050   2       3       0,4070  8
```

9.6.10 One way analysis of Figure 11. A. Evaluation of pSilencer/shRNAcav-1 silencing effect on infection with ZIKV at M.O.I.1 and 24h of post infection time.

```
ANOVA summary
  F     27,08
  P value       < 0,0001
  P value summary       ****
  Are differences among means statistically significant? (P < 0.05)     Yes
  R square      0,8621

Brown-Forsythe test
  F (DFn, DFd)  1,542 (3, 13)
  P value       0,2508
  P value summary       ns
  Significantly different standard deviations? (P < 0.05)       No

Bartlett's test
  Bartlett's statistic (corrected)      25,69
  P value       < 0,0001
  P value summary       ****
  Significantly different standard deviations? (P < 0.05)       Yes

ANOVA table     SS      DF      MS      F (DFn, DFd)    P value
  Treatment (between columns)   2,307   3       0,7690  F (3, 13) = 27,08       P < 0,0001
  Residual (within columns)     0,3692  13      0,02840
  Total 2,676   16

Data summary
  Number of treatments (columns)        4
  Number of values (total)      17
```

```
Number of families      1
Number of comparisons per family        6
Alpha   0,05

Tukey's multiple comparisons test       Mean Diff,      95% CI of diff, Significant?    Summary

  Control  vs. psilencer/shRNAcav-1     0,7932  0,4614 to 1,125 Yes     ****
  Control  vs. ZIKV     0,6344  0,2847 to 0,9842        Yes     ***
  Control  vs. psilencer/shRNAcav-1 ZIKV        1,013   0,6635 to 1,363 Yes     ****
  psilencer/shRNAcav-1 vs. ZIKV -0,1588 -0,4906 to 0,1730       No      ns
  psilencer/shRNAcav-1 vs. psilencer/shRNAcav-1 ZIKV    0,2201  -0,1117 to 0,5519       No      ns
  ZIKV vs. psilencer/shRNAcav-1 ZIKV    0,3789  0,02911 to 0,7286       Yes     *


Test details    Mean 1  Mean 2  Mean Diff,      SE of diff,     n1      n2      q       DF

  Control  vs. psilencer/shRNAcav-1     1,069   0,2759  0,7932  0,1130  4       5       9,923   13
  Control  vs. ZIKV     1,069   0,4347  0,6344  0,1192  4       4       7,529   13
  Control  vs. psilencer/shRNAcav-1 ZIKV        1,069   0,05583 1,013   0,1192  4       4       12,03   13
  psilencer/shRNAcav-1 vs. ZIKV 0,2759  0,4347  -0,1588 0,1130  5       4       1,986   13
  psilencer/shRNAcav-1 vs. psilencer/shRNAcav-1 ZIKV    0,2759  0,05583 0,2201  0,1130  5       4       2,753   13
  ZIKV vs. psilencer/shRNAcav-1 ZIKV    0,4347  0,05583 0,3789  0,1192  4       4       4,496   13
```

9.6.11 One way analysis of Figure 11. B. Same conditions than A, with the difference of an increase viral load, at MOI: 5.

```
ANOVA summary
  F     18,93
  P value       < 0,0001
  P value summary       ****
  Are differences among means statistically significant? (P < 0.05)     Yes
  R square      0,8256

Brown-Forsythe test
  F (DFn, DFd)  22,78 (3, 12)
  P value       < 0,0001
  P value summary       ****
  Significantly different standard deviations? (P < 0.05)       Yes

Bartlett's test
  Bartlett's statistic (corrected)      16,98
  P value       0,0007
  P value summary       ***
  Significantly different standard deviations? (P < 0.05)       Yes

ANOVA table     SS      DF      MS      F (DFn, DFd)    P value
  Treatment (between columns)   2,247   3       0,7491  F (3, 12) = 18,93       P < 0,0001
  Residual (within columns)     0,4748  12      0,03957
  Total 2,722   15

Data summary
  Number of treatments (columns)        4
  Number of values (total)      16


Number of families      1
Number of comparisons per family        6
Alpha   0,05

Tukey's multiple comparisons test       Mean Diff,      95% CI of diff, Significant?    Summary

  Control  vs. psilencer/shRNAcav-1     0,7522  0,3346 to 1,170 Yes     ***
  Control  vs. ZIKV     0,4169  -0,0007424 to 0,8345    No      ns
  Control  vs. psilencer/shRNAcav-1 ZIKV        0,9983  0,5807 to 1,416 Yes     ****
  psilencer/shRNAcav-1 vs. ZIKV         -0,3353 -0,7529 to 0,08226      No      ns
  psilencer/shRNAcav-1 vs. psilencer/shRNAcav-1 ZIKV    0,2461  -0,1715 to 0,6637       No      ns
  ZIKV  vs. psilencer/shRNAcav-1 ZIKV   0,5815  0,1639 to 0,9991        Yes     **


Test details    Mean 1  Mean 2  Mean Diff,      SE of diff,     n1      n2      q       DF

  Control  vs. psilencer/shRNAcav-1     1,069   0,3169  0,7522  0,1407  4       4       7,563   12
  Control  vs. ZIKV     1,069   0,6522  0,4169  0,1407  4       4       4,191   12
  Control  vs. psilencer/shRNAcav-1 ZIKV        1,069   0,07077 0,9983  0,1407  4       4       10,04   12
  psilencer/shRNAcav-1 vs. ZIKV         0,3169  0,6522  -0,3353 0,1407  4       4       3,372   12
  psilencer/shRNAcav-1 vs. psilencer/shRNAcav-1 ZIKV    0,3169  0,07077 0,2461  0,1407  4       4       2,475   12
  ZIKV  vs. psilencer/shRNAcav-1 ZIKV   0,6522  0,07077 0,5815  0,1407  4       4       5,846   12
```

9.6.12 2-WAY ANOVA analysis of Figure 11. C. Evaluation of pSilencer/shRNAcav-1 silencing effect on infection with ZIKV, M.O.I 1 AND 5, using THP-1 transfected cells.

```
Two-way ANOVA   Ordinary
Alpha   0,05

Source of Variation     % of total variation    P value P value summary Significant?
  Interaction   0,1020  0,8788  ns      No
  Row Factor    12,64   0,1017  ns      No
  Column Factor 7,395   0,2039  ns      No

ANOVA table     SS      DF      MS      F (DFn, DFd)    P value
  Interaction   0,02254 1       0,02254 F (1, 19) = 0,02387     P = 0,8788
  Row Factor    2,794   1       2,794   F (1, 19) = 2,958       P = 0,1017
  Column Factor 1,635   1       1,635   F (1, 19) = 1,731       P = 0,2039
  Residual      17,95   19      0,9445
```

9.6.13 T test analysis of Figure 13. A. Study of cav-1 level of expression in infected and transfected cells using pcDNA3/cav-1. MOI: 1 and 24h post infection

```
Column B        pcDNA3/cav-1
vs.     vs,
Column A        Control

Unpaired t test
  P value       0,0035
  P value summary       **
  Significantly different? (P < 0.05)   Yes
  One- or two-tailed P value?   One-tailed
  t, df t=5,083 df=4

How big is the difference?
  Mean ± SEM of column A        1,000 ± 0,02941 N=3
  Mean ± SEM of column B        498,3 ± 97,84 N=3
  Difference between means      497,3 ± 97,84
  95% confidence interval       225,6 to 768,9
  R square      0,8659

F test to compare variances
  F,DFn, Dfd    1,106e+007, 2, 2
  P value       < 0,0001
  P value summary       ****
  Significantly different? (P < 0.05)   Yes

Model comparison        SS      DF      Probability it is correct
  Null H. Population means identical    428369  5       26,34%
  Alternative H: Distinct population means      57432   4       73,66%
  Ratio of probabilities                        2,796
  Difference in AICc                    2,056
```

9.6.14 T test analysis of Figure 13. B. Study of the effect of pcDNA$_3$/cav-1 on ZIKV load, at MOI: 1 and 24h post infection.

```
Column B        pcDNA3/cav-1
vs.     vs,
Column A        Control

Unpaired t test
  P value       0,4612
  P value summary       ns
  Significantly different? (P < 0.05)   No
  One- or two-tailed P value?   One-tailed
  t, df t=0,1037 df=4

How big is the difference?
  Mean ± SEM of column A        1,834 ± 0,7976 N=3
  Mean ± SEM of column B        1,934 ± 0,5383 N=3
  Difference between means      0,09978 ± 0,9622
  95% confidence interval       -2,572 to 2,771
  R square      0,002681

F test to compare variances
  F,DFn, Dfd    2,195, 2, 2
  P value       0,6259
  P value summary       ns
  Significantly different? (P < 0.05)   No

Model comparison        SS      DF      Probability it is correct
  Null H. Population means identical    5,570   5       99,33%
  Alternative H: Distinct population means      5,556   4       0,67%
  Ratio of probabilities                        147,2
  Difference in AICc                    -9,984
```

9.6.15 One way ANOVA analysis for Figure 14. Study of cav-1 level of expression in infected and transfected cells using pcDNA3/cav-1. MOI: 5 and 24h post infection.

```
ANOVA summary
  F     15,87
  P value       0,0010
  P value summary       ***
  Are differences among means statistically significant? (P < 0.05)     Yes
  R square      0,8562

Brown-Forsythe test
  F (DFn, DFd)  2,482 (3, 8)
  P value       0,1352
  P value summary       ns
  Significantly different standard deviations? (P < 0.05)       No

Bartlett's test
  Bartlett's statistic (corrected)
  P value
  P value summary
  Significantly different standard deviations? (P < 0.05)

ANOVA table     SS      DF      MS      F (DFn, DFd)    P value
  Treatment (between columns)   16,75   3       5,582   F (3, 8) = 15,87        P = 0,0010
  Residual (within columns)     2,814   8       0,3517
  Total 19,56   11

Data summary
  Number of treatments (columns)        4
  Number of values (total)      12
```

9.6.16 One way ANOVA analysis for Figure 15 A. Comparison of cav-1 mRNA expression levels between transfected pcDNA3/cav-1 cells, infected or not at MOI: 1, collected after 24h of post Infection time.

```
ANOVA summary
  F     15,05
  P value       < 0,0001
  P value summary       ****
  Are differences among means statistically significant? (P < 0.05)     Yes
  R square      0,6930

Brown-Forsythe test
  F (DFn, DFd)  8,221 (3, 20)
  P value       0,0009
  P value summary       ***
  Significantly different standard deviations? (P < 0.05)       Yes

Bartlett's test
  Bartlett's statistic (corrected)      170,6
  P value       < 0,0001
  P value summary       ****
  Significantly different standard deviations? (P < 0.05)       Yes

ANOVA table     SS      DF      MS      F (DFn, DFd)    P value
  Treatment (between columns)   1,801e+009      3       6,003e+008      F (3, 20) = 15,05       P < 0,0001
  Residual (within columns)     7,978e+008      20      3,989e+007
  Total 2,599e+009      23

Data summary
  Number of treatments (columns)        4
  Number of values (total)      24

  .
  Number of families      1
  Number of comparisons per family        6
  Alpha   0,05

  Tukey's multiple comparisons test       Mean Diff,      95% CI of diff, Significant?    Summary

    Control  vs. pcDNA3/cav-1     -20381  -30587 to -10175        Yes     ****
    Control  vs. ZIKV     -1,400  -10207 to 10205 No      ns
    Control  vs. pcDNA3/cav-1 ZIKV        -12362  -22568 to -2156 Yes     *
    pcDNA3/cav-1 vs. ZIKV 20380   10174 to 30586  Yes     ****
    pcDNA3/cav-1 vs. pcDNA3/cav-1 ZIKV    8019    -2187 to 18225  No      ns
    ZIKV vs. pcDNA3/cav-1 ZIKV    -12361  -22567 to -2155 Yes     *


  Test details    Mean 1  Mean 2  Mean Diff,      SE of diff,     n1      n2      q       DF

    Control  vs. pcDNA3/cav-1     1,000   20382   -20381  3646    6       6       7,905   20
    Control  vs. ZIKV     1,000   2,400   -1,400  3646    6       6       0,0005429       20
    Control  vs. pcDNA3/cav-1 ZIKV        1,000   12363   -12362  3646    6       6       4,794   20
    pcDNA3/cav-1 vs. ZIKV 20382   2,400   20380   3646    6       6       7,904   20
    pcDNA3/cav-1 vs. pcDNA3/cav-1 ZIKV    20382   12363   8019    3646    6       6       3,110   20
    ZIKV vs. pcDNA3/cav-1 ZIKV    2,400   12363   -12361  3646    6       6       4,794   20
```

9.6.17 Mann-Whitney analysis for Figure 15. B. Same conditions than A, with the difference of an increase viral load, at MOI: 5.

```
Column B        pcDNA3/cav-1
vs.     vs,
Column A        Control

Mann Whitney test
  P value       0,0011
  Exact or approximate P value? Exact
  P value summary       **
  Significantly different? (P < 0.05)   Yes
  One- or two-tailed P value?   One-tailed
  Sum of  ranks in column A,B   21,00 , 57,00
  Mann-Whitney U        0,0

Difference between medians
  Median of column A    1,002
  Median of column B    18064
  Difference: Actual    18063
  Difference: Hodges-Lehmann    18063
```

```
Column C        ZIKV
vs.     vs,
Column A        Control

Mann Whitney test
  P value       0,4491
  Exact or approximate P value? Exact
  P value summary       ns
  Significantly different? (P < 0.05)   No
  One- or two-tailed P value?   One-tailed
  Sum of  ranks in column A,C   38,00 , 40,00
  Mann-Whitney U        17,00

Difference between medians
  Median of column A    1,002
  Median of column C    1,076
  Difference: Actual    0,07420
  Difference: Hodges-Lehmann    0,007658
```

```
Column D        pcDNA3/cav-1 ZIKV
vs.     vs,
Column A        Control

Mann Whitney test
  P value       0,0011
  Exact or approximate P value? Exact
  P value summary       **
  Significantly different? (P < 0.05)   Yes
  One- or two-tailed P value?   One-tailed
  Sum of  ranks in column A,D   21,00 , 57,00
  Mann-Whitney U        0,0

Difference between medians
  Median of column A    1,002
  Median of column D    4921
  Difference: Actual    4920
  Difference: Hodges-Lehmann    4920
```

```
Column C        ZIKV
vs.     vs,
Column B        pcDNA3/cav-1

Mann Whitney test
  P value       0,0011
  Exact or approximate P value? Exact
  P value summary       **
  Significantly different? (P < 0.05)   Yes
  One- or two-tailed P value?   One-tailed
  Sum of  ranks in column B,C   57,00 , 21,00
  Mann-Whitney U        0,0

Difference between medians
  Median of column B    18064
  Median of column C    1,076
  Difference: Actual    -18063
  Difference: Hodges-Lehmann    -18063
```

```
Column D        pcDNA3/cav-1 ZIKV
vs.     vs,
Column B        pcDNA3/cav-1

Mann Whitney test
  P value       0,0043
  Exact or approximate P value? Exact
  P value summary       **
  Significantly different? (P < 0.05)   Yes
  One- or two-tailed P value?   One-tailed
  Sum of  ranks in column B,D   55,00 , 23,00
  Mann-Whitney U        2,000

Difference between medians
  Median of column B    18064
  Median of column D    4921
  Difference: Actual    -13142
  Difference: Hodges-Lehmann    -11585
```

```
Column D        pcDNA3/cav-1 ZIKV
vs.     vs,
Column C        ZIKV

Mann Whitney test
  P value       0,0011
  Exact or approximate P value? Exact
  P value summary       **
  Significantly different? (P < 0.05)   Yes
  One- or two-tailed P value?   One-tailed
  Sum of  ranks in column C,D   21,00 , 57,00
  Mann-Whitney U        0,0

Difference between medians
  Median of column C    1,076
  Median of column D    4921
  Difference: Actual    4920
  Difference: Hodges-Lehmann    4920
```

critical value:	0,05	number of tests:	3
		corrected critical value:	0,05

Labels	P-values	Bonferroni-corrected significance	Bonferroni-corrected P-value
pcDNA3/cav-1 ZIKV	0,0011	significant	0,0033
pcDNA3/cav-1	0,0011	significant	0,0033
ZIKV	0,4491	not significant	1

9.6.18 Two way ANOVA analysis for Figure 15. C. Study of the effect of pcDNA$_3$/cav-1 on ZIKV load, at MOI: 1 and 5 and 24h of post infection time

```
Two-way ANOVA   Ordinary
Alpha   0,05

Source of Variation     % of total variation    P value P value summary Significant?
  Interaction   33,54   0,0243  *       Yes
  Row Factor    5,829   0,2950  ns      No
  Column Factor 6,890   0,2573  ns      No

ANOVA table     SS      DF      MS      F (DFn, DFd)    P value
  Interaction   1,812   1       1,812   F (1, 10) = 7,026       P = 0,0243
  Row Factor    0,3149  1       0,3149  F (1, 10) = 1,221       P = 0,2950
  Column Factor 0,3723  1       0,3723  F (1, 10) = 1,443       P = 0,2573
  Residual      2,579   10      0,2579


Compare each cell mean with the other cell mean in that column.

Number of families      1
Number of comparisons per family        2
Alpha   0,05

Sidak's multiple comparisons test       Mean Diff,      95% CI of diff, Significant?    Summary

  MOI 1 - MOI5
    pcDNA3      0,4388  -0,5043 to 1,382        No      ns
    pcDNA3/cav-1        -1,066  -2,221 to 0,08888        No      ns


Test details    Mean 1  Mean 2  Mean Diff,      SE of diff,     N1      N2      t       DF

  MOI 1 - MOI5
    pcDNA3      1,657   1,219   0,4388  0,3591  4       4       1,222   10
    pcDNA3/cav-1        1,246   2,312   -1,066  0,4398  2       4       2,424   10
```